Diploma thesis

Laboratory diagnostics of rhinoliquorrhea and its evaluation

Written by

Vadim Vershinin

submitted in partial fulfillment of the requirement for the degree of

Doctor of medicine

(Dr. med. univ.)

at the

Medizinische Universität Graz

performed at

Universitätsklinik für Neurologie

under supervision of

Assoz. Prof.in Priv.-Doz.in Dr.in med.univ. Dr.in rer.nat. Sonja Hochmeister

Dr.in scient.med. Michaela Haindl, BSc MSc

Graz 30.09.2021

Eidesstattliche Erklärung

Ich erkläre ehrenwörtlich, dass ich die vorliegende Arbeit selbstständig und ohne fremde Hilfe verfasst habe, andere als die angegebenen Quellen nicht verwendet habe und die den benutzten Quellen wörtlich oder inhaltlich entnommenen Stellen als solche kenntlich gemacht habe.

Graz, am 30.09.2021 *Vadim Vershinin eh*

Acknowledgements

First of all, I would like to express my gratitude to all the laboratory team, study office of neurology clinic and especially to both my mentors, Frau Assoz. Prof.in Priv.-Doz.in Dr.in med.univ. Dr.in rer.nat. Hochmeister and Frau Dr.in scient.med. Michaela Haindl, BSc MSc, for their kindness, patience and of course for comprehensive support during writing this diploma thesis. I cannot overestimate your help, efforts and time you've spent. I appreciate experience and knowledge I've gained being under your guidance.

Life is not always a pleasant journey and sometimes you're on a black line. In such moments it's important to have people nearby to rely on. I'm thankful to my family and friends being on my back no matter what.

I'm happy, I've met all those people on my way, their kindhearted support helped me to achieve such meaningful goal.

List of content

List of tables

List of figures

Abbreviations

ABC - ATP-binding cassette

ACE - angiotensin converting enzyme

AJ - adherens junctions

ANP - atrial natriuretic peptide

ATP - adenosine triphosphate

AUC – area under the curve

BBB - blood-brain barrier

BCRP - breast cancer-resistance protein

BCSFB - blood-cerebrospinal fluid barrier

BTP - ß-trace-protein

CNS - central nervous system

COX - cyclooxygenase

CPP - cerebral perfusion pressure

CSF - cerebrospinal fluid

ENT – otolaryngology

GFR – glomerular filtration rate

GLUT - Glucose transporter

HF - hemofiltrate

HRCT - high-resolution computer tomography

ICP - intracranial pressure

JAMs - junctional adhesion molecules

L-CSF - lumbar cerebrospinal fluid

LDL - low density lipoproteins

MAGUK - membrane-associated guanylate kinase-like family

MAP - mean arterial pressure

MCTs - monocarboxylate transporters

MDR - multidrug-resistance protein

MRP - multidrug resistance-related protein

NPV – negative predictive value

NSE - neuron-specific enolase

OC(A)Ts - amino acid transporters, peptide transporters, organic cation and anion transporters

Pg – prostaglandin

PPV – positive predictive value

ROC – receiver operating characteristic

s-ICAM - soluble intercellular adhesion molecule

SLC - solute carrier

TEER - transepithelial/transendothelial electrical resistance

TJ - tight junctions

TTR - transthyretin

V-CSF - ventricular cerebrospinal fluid

VLDL - very low density lipoproteins

ZO - zonula occludens

Zusammenfassung

Einleitung

Die Rhinoliquorrhoe ist ein klinischer Zustand, bei dem der Liquor über eine pathologische Verbindung von der Schädelhöhle im Bereich der vorderen oder mittleren Schädelgrube in die Nase austritt. Vom ätiologischen Standpunkt unterschiedet man traumatische und nicht traumatische Liquorfisteln. Eine der gefährlichsten damit verbundenen Komplikationen ist die bakterielle Meningitis, daher ist eine sichere und schnelle Diagnosestellung essentiell. Für diesen Zweck kommen radiologische und laborchemische Methoden zum Einsatz. Die Diagnostik kann sich jedoch herausfordernd gestalten, da die Größe des Lecks eine potentielle Einschränkung in der radiologischen Bildgebung darstellt. Dementsprechend kann bei Verdacht auf Liquorrhoe eine Analyse des Nasenausflusses auf liquorspezifische Komponenten in Erwägung gezogen werden.

Unter allen gehirnspezifischen Komponenten, die im Liquor zu finden sind, ist das ß Trace Protein (BTP) von besonderem Interesse. Es ist ein Protein mit einer auffallend hohen intrathekalen Fraktion sowie CSF/Serum-Ratio. Außerdem zeigt es eine relativ hohe Konzentration im Liquor. Die empfohlenen cut-off Werte in der Analyse des Nasenausflusses variieren in der Literatur jedoch derzeit zwischen 0.244 und 6 mg/l. Das Hauptziel dieser Diplomarbeit ist, die diagnostische Genauigkeit bei der Bestimmung eines Liquorlecks zu verbessern, sowie die existierenden BTP cut-off Werte neu zu evaluieren. Das zweite Ziel war die retrospektive Berechnung von Sensitivität und Spezifizität mittels NPV und PPV.

Methoden

Die BTP Konzentrationen in V-CSF (Ventrikelliquor) und L-CSF (lumbal gewonnener Liquor), (n = 24 für jede Gruppe), und im Nasenausfluss von gesunden Freiwilligen (n = 17) wurden unter Beimischung von schrittweise verdünnter (rein, 2-, 3- und 4-Fach) V- oder L-CSF mittels Nephelometrie gemessen.

Um BTP als passende Methode zu evaluieren, wurden die BTP Konzentrationen im Serum (n = 17), im Nasenausfluss für die Bestimmung der BTP-Konzentrationen der gesunden Stichproben (n = 188) und der Nasenausfluss von operativ untersuchten Patienten (n = 75) statistisch analysiert.

Da der Kolmogorov-Smirnov Test in einigen Gruppen keine Normalverteilung zeigte, wurde die statistische Evaluierung mithilfe nicht parametrischer Tests durchgeführt. Für die Bestimmung der Signifikanz zwischen den Gruppen wurden der Kruskal-Wallis und der Mann-Whitney-U-Test verwendet; für die Untersuchung der Korrelationen wurde der Korrelationskoeffizient nach Spearman berechnet. Der BTP cut-off Wert im Nasenausfluss wurde via ROC Kurve bestimmt. Sensitivität, Spezifizität sowie positive und negative prädiktive Werte wurden mittels Kreuztabelle kalkuliert.

Ergebnisse

Es wurde sowohl ein signifikanter Unterschied ($p < 0,001$) zwischen den Mittelwerten der BTP-Konzentrationen von V-CSF (10,94 mg/l) und L-CSF (25,69 mg/l), als auch zwischen den BTP-Konzentrationen von Serum (0,52 mg/l) und Nasenausfluss (0,29 mg/l) detektiert. Mittels Korrelationskoeffizient nach Spearman konnte eine inverse Korrelation ($p < 0,001$) zwischen den verdünnten Proben festgestellt werden. Die ROC Kurve (Figure 17) zeigte eine AUC von 0.765 mit einer Signifikanz von $p < 0,001$. Zusätzlich konnten eine Sensitivität von 100% mit dem PPV von 75,7% und eine Spezifizität von 22,7% mit dem NPV von 100% beschrieben werden ($p < 0,001$).

Konklusion

Die Ergebnisse dieser Studie unterstützen den aktuellen cut-off Wert von 1,3 mg/l.

Zusammenfassend scheint das BTP ein verlässlicher Marker zur Detektion einer auch geringen Rhinoliquorrhoe zu sein. Dieser bedarf jedoch weiterer Evaluierung unter Berücksichtigung potentieller Limitationen. Bestimmte patientInnenbezogene Faktoren, wie beispielsweise eine bakterielle Meningitis, Niereninsuffizienz oder multiple Schädelverletzungen können zu einer Veränderung der BTP-Werte in der jeweiligen Probe führen. Die Beurteilung muss daher immer auch im klinischen Kontext gesehen werden.

Abstract

Objective

Rhinoliquorrhea is a clinical condition, where cerebrospinal fluid (CSF) passes through the nose via a pathological connection to the cranial cavity in the area of anterior or middle cranial fossa. From etiological point of view, traumatic, iatrogenic and spontaneous CSF fistulas can be distinguished. One of the most dangerous related complications is bacterial meningitis, thus an accurate and fast diagnosis is important. For this purpose, radiological and laboratory methods are used. However, diagnostics can be quite challenging, since a small defect size is a limitation to radiological methods. Accordingly, nasal discharge analysis to examine CSF specific compounds seems to be a suitable prospective method.

Among all CSF proteins, ß- trace protein (BTP) is most interesting. It is a protein with impressively high intrathecal fractions, CSF/Serum ratio and shows relatively high concentrations in CSF. However, recommended cut-off values in the literature vary widely between 0.244 and 6 mg/l. The main aim of this diploma thesis is to improve the diagnostic accuracy of determining CSF leakage and new evaluation of existing cut-off values in nasal discharge. A second aim was the retrospective calculation of specificity and sensitivity using NPV and PPV.

Methods

BTP concentrations in ventricular CSF (V-CSF) and lumbar CSF (L-CSF), (n = 24 each), and in nasal discharge from known healthy volunteers (n = 17) with admixture of gradually prediluted (pure, 2, 3 and 4 Fold) V- or L-CSF was measured via nephelometry.

In order to evaluate BTP as a suitable marker, BTP concentrations in serum (n=17), nasal discharge for determining BTP concentration of healthy population (n = 188) and nasal discharge of operative examined patients (n = 75) were statistically analyzed.

Since some groups revealed to be not normally distributed (evaluated via Kolmogorov-Smirnov test), non-parametric tests were preferred. For determining the significance between groups, Kruskal-Wallis and Mann-Whitney-U-Test were used; for investigation of correlations, Spearman's correlation coefficient was calculated. BTP cut-off value in nasal discharge was determined via ROC Curve. Sensitivity, specificity, positive and negative predictive values were calculated via cross tables.

Results

There was a significant difference ($p < 0.001$) detectable between the means of V-CSF (10.94 mg/l) and L-CSF (25.69 mg/l) BTP concentrations, as well as serum (0.52 mg/l) and nasal discharge (0.29 mg/l) values. An inverse correlation between prediluted samples was detected via Spearman's correlation coefficient ($p < 0.001$). The ROC curve (Figure 16) represented an AUC of 0.765 with a significance of $p < 0.001$. Additionally, a sensitivity of 100% with a PPV of 75.7% and a specificity of 22.7% with a NPV of 100% could be described ($p < 0.001$).

Conclusion

The results of this study suggest the acceptance of the cut-off value of 1.3 mg/l.

We conclude that BTP seems to be a promising laboratory marker of even minor rhinoliquorrhea, which however requires further evaluation with consideration of possible limitations. Certain patient related features like bacterial meningitis, impaired renal function and multiple skull injuries can lead to BTP value changes in the respective sample. Thus, evaluation must always been done considering the clinical context.

1. Introduction

1.1. Basic Anatomy

1.1.1. Skull Base

The skull base is an anatomical structure with close interaction of bones and soft tissues. The bone part includes frontal, temporal, ethmoid, sphenoid and occipital bones and is anatomically divided into three compartments (fossae) – anterior, middle (central) and posterior fossa (Figure 1). Numerous foramina allow neurovascular formations of the brain to reach their target organs [40, 38, 23].

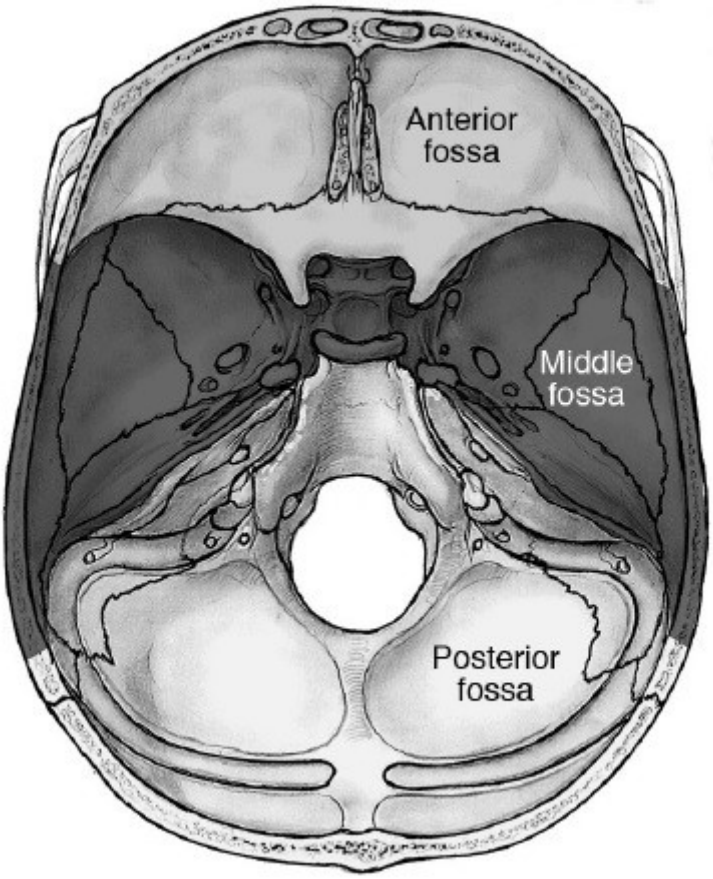

Figure 1. Cranial base

Anatomy of the Skull Base and Related Structures: Elements of Surgical Anatomy. Neupsy Key, 18.02.2017

1.1.1.1. Anterior Cranial Fossa

The anterior cranial fossa (Figure 2) consists of frontal, sphenoid and ethmoid bones. There are four borders to be distinguished:

1) The anterolateral border is formed by the internal surface of the frontal bone.
2) The posteromedial border is formed by a limbus of the sphenoid bone.

3) The posterolateral border is formed by the lesser wing of the sphenoid bone.
4) The inferior part consists of the orbital parts of the frontal bone, cribriform plate and crista galli of the ethmoid bone, the body and the lesser wing of the sphenoid bone.

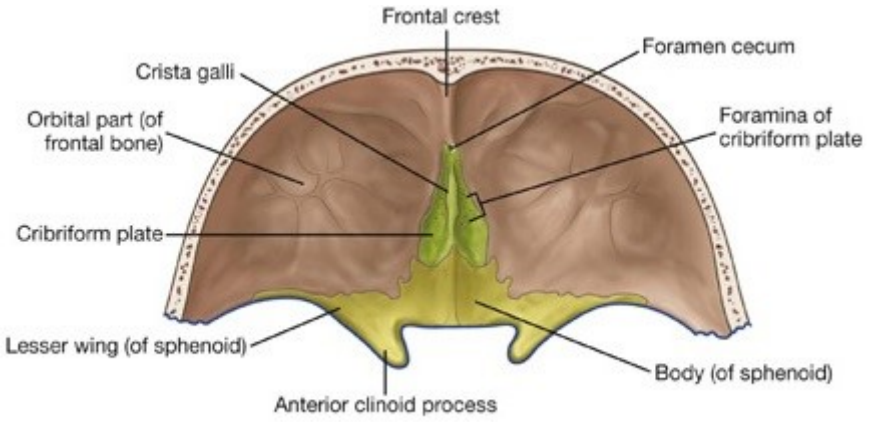

Figure 2. Anterior cranial fossa

Drake R. L. et al. Gray's Anatomy for Students 4th Edition. Elsevier, 2020. 853.

The frontal bone separates the cranial cavity from the orbit, nasal cavity and frontal sinus. Through the thin and rather vulnerable cribriform plate, olfactory nerves pass into to the nasal cavity. Through the foramen caecum, located on the upper nasal part of the frontal bone, emissary veins go to sinus sagittalis during childhood; however, in adults this foramen is closed. The optic canal is located in the lesser wing of the sphenoid bone; ophthalmic nerve and artery pass through it. [40, 38, 23]

1.1.1.2. Middle Cranial Fossa

The middle cranial fossa (Figure 3) is formed by the sphenoid and temporal bone. There are five borders to be distinguished:

1) The anterolateral border is formed by the lesser wings of the sphenoid bone.
2) The anteromedial border is formed by the limbus of the sphenoid bone.
3) The posterolateral border is bounded by the superior border of the petrous part of the temporal bone.
4) The posteromedial border is formed by the sellae of the sphenoid bone.
5) The inferior part consists of the body and greater wings of the sphenoid bone, squamous and petrous parts of the temporal bone.

The ophthalmic, oculomotor, trochlear and abducens nerves, as well as the superior and inferior ophthalmic veins pass through the superior orbital fissure. The ophthalmic artery and optic nerve pass through the optic nerve canal. Foramen ovale surrounds the mandibular nerve and accessory meningeal artery, the foramen spinosum sheath the middle meningeal artery and the meningeal branch of the mandibular nerve. The vidian canal allows the vidian nerve, artery and vein to pass, while Meckel's canal is reserved for trigeminal nerve ganglion.

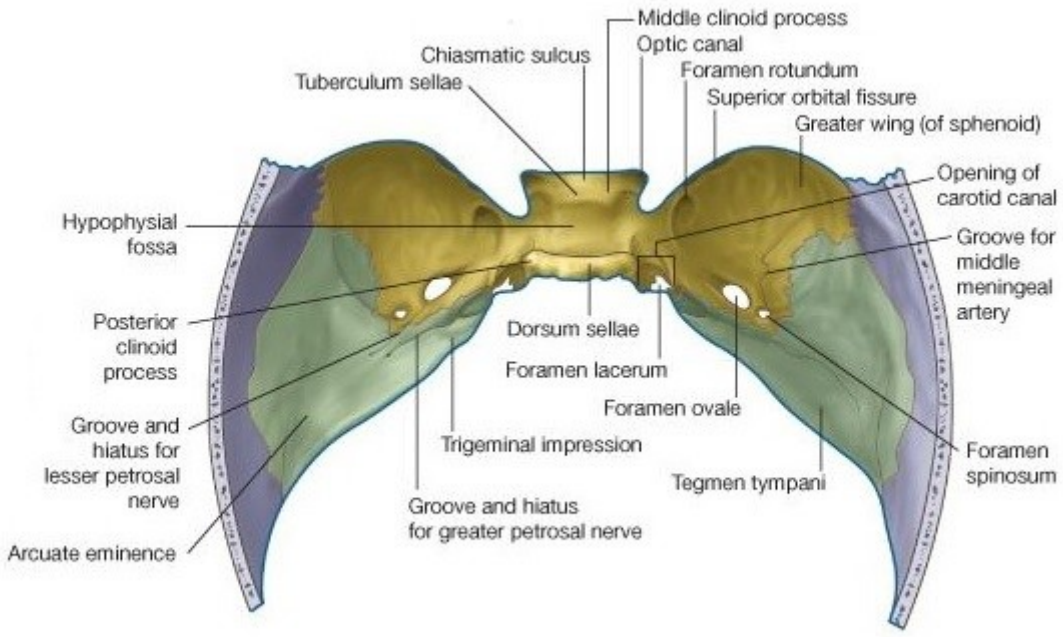

Figure 3. Middle cranial fossa

Drake R. L. et al. Gray's Anatomy for Students 4th Edition. Elsevier, 2020. 855.

1.1.1.3. Posterior Cranial Fossa

The posterior cranial fossa (Figure 4) is formed by temporal and occipital bones with the following borders:

1) The anterior boundary is formed by superior petrous of the temporal bone.
2) The posterior part is formed by the lesser part of the squamous tissue of the temporal bone.
3) The lateral side consists of the temporal and the occipital bones.
4) The inferior part is formed by the occipital bones.

The temporal bone includes the following structures:

1) The internal auditory meatus paves the way for facial, vestibulocochlear nerves and labyrinthine artery.
2) The facial nerve canal.
3) The petrous carotid canal for petrous segment of the internal carotid artery.

The occipital bone contains these structures:

1) The foramen lacerum transmits the artery of pterygoid canal, emissary veins and the anterior part of the vidian nerve.
2) The jugular foramen serves as path for glossopharyngeal, vagus and spinal accessory nerves as well as for the inferior petrosal sinus and the jugular bulb.
3) The foramen magnum connects the skull with the spinal canal and contains the medulla oblongata. Furthermore, vertebral, anterior and posterior spinal arteries pass through this opening.
4) The hypoglossal canal is a path for the hypoglossal nerve [40, 38, 23].

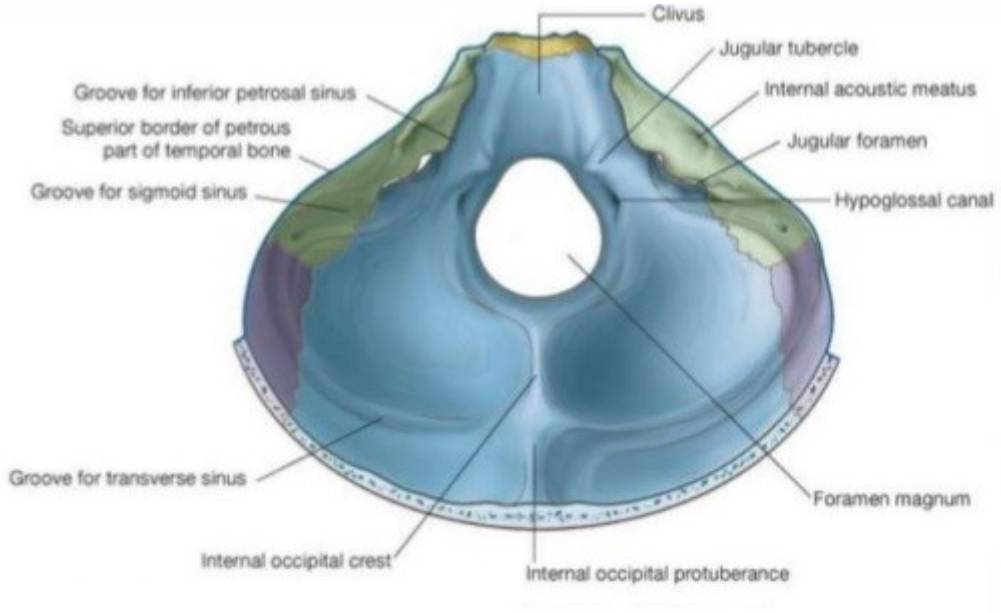

Figure 4. Posterior cranial fossa

Drake R. L. et al. Gray's Anatomy for Students 4th Edition. Elsevier, 2020. 857.

1.2. Cerebrospinal fluid (CSF)

CSF is a clear, colorless substance that constantly circulates in the ventricles of the brain and subarachnoidal space. Its amount is highly variable due to age or pathological conditions that enlarge external and/or internal CSF spaces; in young healthy individuals a total volume of 150 ml CSF (125 ml in the subarachnoid space; 25 ml filling the

ventricles), creating a pressure of 10-15 mmHg, can be expected. It exerts a variety of essential functions, a selection is listed below [24, 8, 47]:

1) Hydromechanical protection of the central nervous system. This function is carried out via two mechanisms. One of them is the ability for shock wave absorbance of the CSF. Furthermore, CSF makes the brain buoyant, which leads to effective weight reduction up to 97% (from 1400-1500 grams to 45-50 grams).
2) CSF maintains homeostasis of the interstitial fluid through providing nutrients and hormones and removing waste products of the brain metabolism.
3) CSF regulates the intracranial pressure (ICP). The cerebral perfusion pressure (CPP) results from ICP and arterial blood pressure. The CPP is responsible for brain blood flow; its normal values vary between 50 and 70 mmHg [67]. The CPP as well as the ICP are strictly controlled under physiological conditions, as uncontrolled fluctuations can easily lead to tissue damage. [68]
   The CPP can be calculated using the following formula:
   CPP = MAP – ICP; where MAP is the mean arterial pressure [34].

To carry out all of these functions properly, synthesis and circulation of CSF is highly regulated. This system can be divided into two parts constantly interacting with each other: the external and the internal CSF spaces.

1.2.1. CSF spaces and CSF circulation

The external (or subarachnoidal) CSF space is located between the arachnoidea mater and pia mater. The internal CSF space is formed by the ventricles of the brain and the central canal of the spinal cord, extending to the S2 vertebra. The external CSF space is accompanied by a certain number of expansions, so called Cisternae subarachnoideae:

1) Cisterna cerebellomedullaris
2) Cisterna pontocerebellaris
3) Cisterna interpeduncularis
4) Cisterna ambiens
5) Cisterna chiasmatica
6) Cisterna lumbalis

1.2.1.1. Ventricles

The ventricular system is presented in Figure 5. The internal side of ventricles is covered with ependymal cells that have special microcilia on their surface, which are responsible for CSF dynamics.

1.2.1.1.1. Lateral ventricle

Lateral ventricles are paired, C-shaped formations in both hemispheres of the brain respectively (also distinguished in left and right ventricles). In each ventricle the following formations occur:

1) The body, the central part of the ventricle.
2) The anterior horn extends into the frontal lobe, providing connection with the 3rd ventricle through the interventricular foramen.
3) The posterior horn extends into the occipital lobe.
4) The inferior horn, the largest horn, extending into the temporal lobe, and the only horn that has a connection with the choroid plexus.

1.2.1.1.2. 3rd ventricle

The 3rd ventricle is located between both thalami. Frontally, this structure is connected with the lateral ventricles through the foramen interventriculare and postrioinferiorly the 3rd ventricle communicates with the 4th ventricle through the aqueductus mesencephali. The following parts describe the 3rd ventricle: a roof, a floor and walls (anterior, posterior and two lateral walls).

1) The anterior wall is formed by anterior columns of fornix, anterior commissure and lamina terminalis.
2) The posterior wall is formed by pineal gland, posterior commissure and cerebral aqueduct.
3) Lateral walls consist of a larger part (medial surface of the anterior two-thirds of the thalamus) and a smaller part (hypothalamus).
4) The floor is formed by optic chiasma, tuber cinereum and infundibulum, mammillary body, posterior perforated substance and tegmentum of the midbrain.
5) The roof is formed by a sheet of ependyma, which is covered by a triangular fold of the pia mater, forming the choroid plexus of the 3rd ventricle.

1.2.1.1.3. 4th ventricle

The following parts describe the 4th ventricle:

1) The lateral wall is inferolaterally formed by gracile and cuneate tubercles and inferior cerebellar peduncles. Superolaterally the wall is formed by the superior cerebellar peduncle.
2) The floor consists of three parts: upper (posterior surface of the pons), intermediate (base of the upper triangular part above and by a line joining the taenia below) and lower part (posterior surface of the upper medulla).
3) The cephalic portion of the roof is formed by 2 superior cerebellar peduncles and a thin sheet of white matter, called superior medullary velum, bridges the gap between them. The lower half of the roof is covered by the inferior medullary velum, which is formed by the ventricular ependyma and the tela choroidea (a double layer fold of pia mater) of the fourth ventricle. The 2 layers of tela choroidea enclose the choroid plexus of the fourth ventricle in the form of vascular fringes.

The 4th ventricle is connected with the third ventricle through the aqueductus mesencephali and caudally to the canalis centralis of the spinal cord. Furthermore, the 4th ventricle is connected through the apertura mediana (Magendii) with the cisterna cerebellomedullaris und through both aperturae lateralis (Luschkae) with the cisterna pontocerebellaris, and via those structures, with the external CSF spaces. [8, 53]

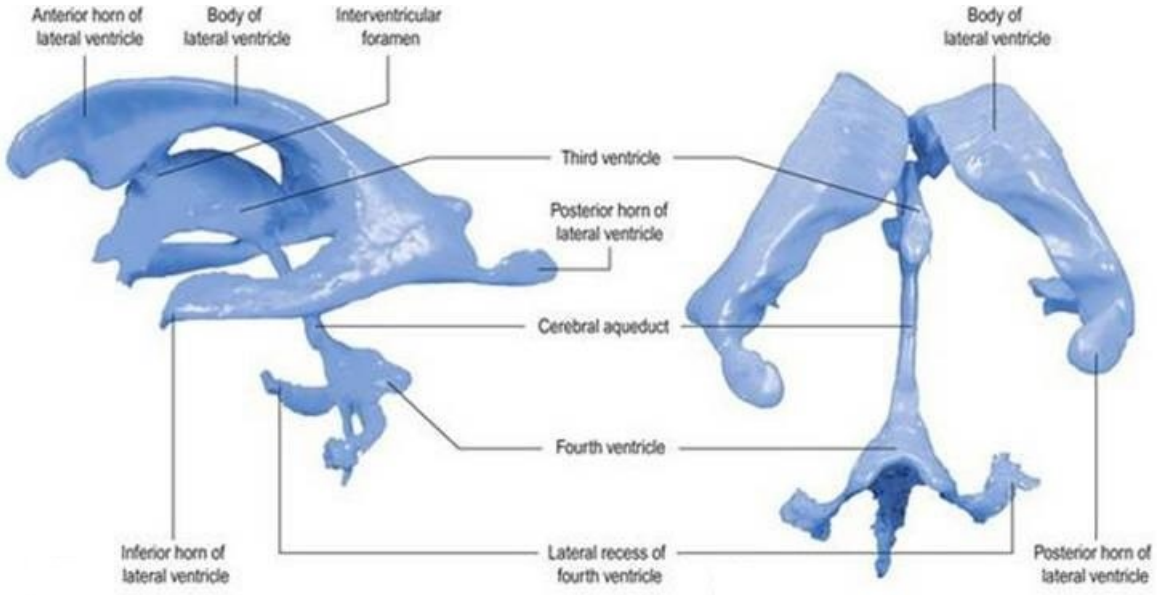

Figure 5. Ventricular system

1.2.1.1.4 Choroid plexus

The choroid plexus is the main site of CSF production and consists of two parts [8]:

1) Tela choroidea, consisting of connective tissue with fenestrated capillaries.
2) Plexus epithelium: special ependymal cells that are responsible for liquor production, playing an outstanding role for the barrier function by forming the blood-CSF barrier (BCSFB). They are also covered with microcilia, facilitating liquor dynamics. [16]

1.2.2. Cerebrospinal fluid production

CSF is renewed about 5 times a day, although with ageing this rate decreases down to 3 times in 24 hours by the age of 77 years. During a period of 24 hours, around 400-600 ml of CSF are produced [47]. A huge part of that amount, 70%, is produced by the plexus choroideus of ventricles. There is also another, extrachoroidal source of CSF production: extracellular fluid, cerebral capillaries and the ependymal epithelium; but these pathways play a minor role under physiological conditions.

1.2.2.1. Choroidal secretion

The choroidal secretion occurs in two steps. The first step is a passive filtration of plasma through the wall of the choroid capillaries into the choroid intracellular space. The second step is an active transfer of required compounds by selective transporters. The main mechanism of active transport mainly occurs through ion exchange. An outstanding role in this pathway plays an enzyme called cytoplasmic carbonic anhydrase. It implements the reaction between H_2O and CO_2 resulting in the formation of H^+ and HCO_3^- ions. The carrier proteins exchange these ions for Na^+ and Cl^- from interstitial space, followed by ATP-dependent ion pump excretion of Na^+, Cl^-, HCO_3^- and K^+ to the intraventricular lumen. As a result, the osmotic gradient forces water to stream in through the aquaporin I channels [47, 18].

1.2.2.2. Regulation of secretion and composition

There is a variety of factors that can influence the dynamics of CSF secretion and its composition [47, 18]:

1) Intraventricular pressure. With the increase of intraventricular pressure, the gradient between pressure in capillaries and choroid plexus interstitia falls and thereby decreases the amount of filtration.
2) Arterial blood pressure. Hypotension leads to reduced choroidal perfusion pressure, which lowers CSF production.
3) Innervation: The choroid plexus is influenced by different parts of the nervous system: cholinergic, adrenergic, serotoninergic and peptidergic system; each of them resulting in different effects. The sympathetic system reduces secretion, the cholinergic system in contrast increases secretion. The autonomic nervous system is furthermore responsible for circadian rhythm of secretion.
4) Humoral regulation. Acidity of environment can regulate the activity of some important factors like carbonic anhydrase, aquaporins and Na-K-Cl transporters.
5) Monoamine and neuropeptide. In experiments, it was demonstrated, that 5-HTP also reduces CSF production [35]. Atrial natriuretic peptide and arginine vasopressin decrease CSF secretion, as ANP acts through aquaporin I. Dopamine and melatonin can also influence CSF dynamics [47].

1.2.3. CSF circulation

The circulation of CSF is characterized by the positional flow, following systolic contractions, in direction from the place of secretion, the lateral ventricles, then through the intraventricular foramen to the 3rd ventricle, the aqueductus mesencephali on its way to the 4th ventricle. Finally, it flows into the canalis centralis of the spinal cord or to the subarachnoid space through the median and the 2 lateral aperturae.

1.2.4. CSF absorption

The main site of absorption of CSF are the arachnoid villi, which are convex structures of the endothelium. For the absorption a pressure gradient ranging between 3-5 mmHg is essential. Spinal arachnoid villi lead to the cranial subarachnoidal space. Cranial villi connect the subarachnoidal space and the venous sinuses where the CSF is mixed with blood and exits through the cranial veins.

Furthermore, extra-arachnoid absorption sites of the CSF can be described:

1) Some of those absorption sites can be found along cranial and spinal nerve sheaths.
2) CSF elimination also takes place in interstitial compartments via Virchow-Robin perivascular spaces.

3) Another absorption site is located in meningeal sheaths.
4) Absorption also occurs along spinal and cranial nerve roots.
5) Furthermore, CSF can be absorbed in the region of cribriform plate of the ethmoid bone.
6) Finally, the glymphatic pathway plays an important role in CSF absorption. It consists of three parts: the paraarterial routes of the fluid, fluid flow facilitated through aquaporin 4 channels and the paravenous routes, which drain the CSF ultimately to the subarachnoid CSF, blood stream or meningeal lymphatic vessels [47, 19, 60].

1.2.5. CSF composition

Because of the wide range of essential functions which are fulfilled by the CSF, it has a constantly controlled composition of fluid, ions and proteins.

The ionic content is comparable with the one in plasma (the concentration is measured in mmol/kg H_2O) whereas glucose concentration (50-75 mg/dl) and pH (7.3) are slightly lower [19, 66]:

- Na^+ 149.0
- K^+ 3.0
- Ca^+ 1.0
- Mg^+ 1.0
- Cl^- 128.0
- Phosphat$^-$ 0.6
- Lactat$^-$ 1.3
- HCO_3^- 26.0

The CSF also contains a fraction of proteins that can be divided into two groups: blood-derived proteins and brain-derived proteins. The former are produced outside the brain and penetrate through the BCSFB. For example, albumin, IgG, IgA and IgM can be attributed to this type of proteins.

Brain-derived proteins are characterized by their high concentration in CSF in comparison to their serum presence. They are divided into three groups according to their origin [44]:

1) Neuronal and glial cell origin: S-100 B, tau-protein, neuron-specific enolase (NSE)
2) Leptomeningeal origin: ß-trace-protein (BTP), cystatin C

3) Proteins with non-negligible blood-derived fraction: transthyretin, angiotensin converting enzyme (ACE), soluble intercellular adhesion molecule (s-ICAM)

Table 1. Protein concentration in lumbar CSF and their intrathecal fraction.

Protein	MW in kDa	CSF concentration	CSF/serum ratio	Intrathecal fraction (%)
ß-Trace-Protein	25	16.6 mg/ml	34:1	>99
Cystatin C	13.3	3.1 mg/l	5:1	>99
Tau-Protein	55-74	0.2 µg/l	10:1	>99
S-100 B	21	1.5 µg/l	18:1	>99
NSE	78	8 mg/l	1:1	>99
Transthyretin	55	17 mg/l	1:18	>90
ACE	150	-	1:100	>65
s-ICAM	90	1.5 µg/l	1:190	>30
Albumin	67	245 mg/l	1:205	0
IgG	150	25 mg/l	1:440	0
IgA	170	1.0 mg/l	1:800	0
IgM	900	0.2 mg/l	1:3400	0

With up to 80% the most frequent proteins in CSF are blood-derived ones, particularly albumin despite an existing BBB and BCSFB (see Table 1).

1.3. Barrier between blood and CSF

To keep all these indicators in required ranges, there must be a special anatomical prerequisite. This system is called blood-CSF barrier (BCSFB). Its main function is to keep undesirable substances, which are present in the blood, away from CSF. Moreover, BCSFB selectively allows the transportation of important compounds through different mechanisms.

1.3.1. BCSFB structure

Anatomically, the BCSFB is located in the choroid plexus. In contrast to the BBB, BCSFB consists of fenestrated “open” capillaries and one layer of epithelial cells that cover the intraventricular side of choroid plexus, forming the barrier function. On molecular level

this function is provided through apical-located intracellular contacts: tight junctions (TJ), adherens junctions (AJ); and active transporters.

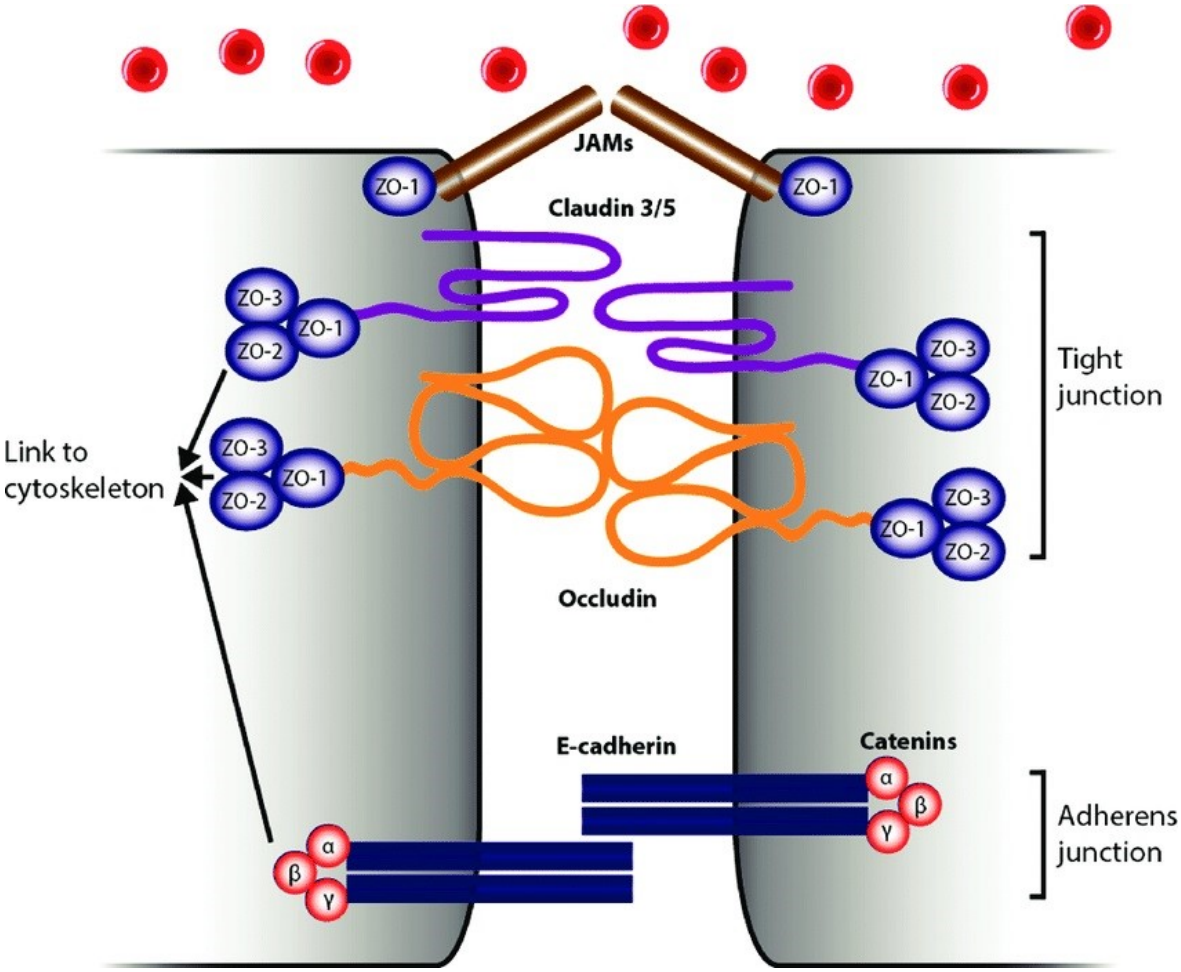

Figure 6. Tight and adherens junctions structure

Dickens D. et al. Drug transporters at the blood-brain barrier. Drug Transporters: Volume 1: Role and Importance in ADME and Drug Development. The Royal Society of Chemistry, 01.2016. 155.

1.3.1.1. Intracellular contacts

1.3.1.1.1. Tight junctions

Structurally TJs are combinations of two groups of proteins:

1) Transmembrane proteins: occludin, claudin and junctional adhesion molecules (JAMs). They form not only a physical barrier, but also a transepithelial/transendothelial electrical resistance (TEER), which repels specific compounds.
2) Intracellular scaffolding proteins from membrane-associated guanylate kinase-like family (MAGUK): zonula occludens (ZO).

Interaction of these groups of proteins creates a special complex, connected with the actin-based cytoskeleton, which forms pores and realize passage for definitive molecules [26, 49, 51].

Two functions of TJs can be distinguished:

1) The gate function implicates transport regulation of soluble compounds and ions through the cell membrane. Substances with high octanol/water partition coefficient, lipophilic molecules with less than 8-H-bonds and 400 Da can easily diffuse into CNS, while molecules with low coefficients can only pass to CNS via active transporters [26, 58, 33].
2) The fence function limits a free movement of lipids and proteins from the apical to the basal part of the cell, maintaining cell polarity by preventing mixing molecules from different parts of the cell [58, 51].

1.3.1.1.1.1. Transmembrane Proteins

1.3.1.1.1.1.1. Occludin

Occludin is a monomeric protein with a molecular weight of 60-65 kDa, which forms dimers in contact with cells. It consists of 2 extracellular loop-shaped domains, 4 intracellular and 3 cytoplasmatic domains [26, 49, 28]. Occludins first loop controls gate function and the second loop is responsible for TEER in values of about 150 Ω cm^2 [41]. Occludins C-terminus connects with the GK domain of the ZO, which in its turn binds with the cytoskeleton providing their interactions [26]. Its N-terminus is responsible for TEER-formation. Occludin is also associated with a range of intracellular G-proteins, responsible for endocytosis and recycling of Occludin [41].

1.3.1.1.1.1.2. Claudin

Claudins are a family of proteins with 24 different types and range in their molecular weight between 20-27 kDa. Claudins consist of 2 extracellular loops, 4 transembrane domains and an intracellular C-terminus that binds with the PDZ domain of ZOs. Even though 24 types of this protein are found in humans, in BCSFB TJs only a few of them are present: claudin-1 regulates the para-cellular movement of macromolecules, claudin-2 is a pore-forming protein with a high selectivity to Na^+ and K^+ especially during brain development and claudin-3 is responsible for barrier genesis [56, 58, 20].

1.3.1.1.1.1.3. Junctional Adhesion Molecules

JAMs belong to the immunoglobulin family, and have a molecular weight of 40 kDa. There are three structural domains to be described: an extracellular domain with two loops, a transmembrane domain and a short intracellular tail that binds with the PDZ domain ZO. JAMs can be divided into three groups: JAM-A plays a role in BBB maintenance, JAM-B is responsible for leukocyte trafficking in skin endothelium, and JAM-C is located in BCSFB and controls CSF homeostasis [26, 58].

1.3.1.1.1.2. Intracellular scaffolding proteins

1.3.1.1.1.2.1. Zonula Occludens

ZO belongs to the membrane-associated guanylate kinase homologs (MAGUK) family. It connects TJ and AJ proteins with the cytoskeleton. ZO consists of several domains: three PDZ, one SH3 and guanylat-kinase domain, respectively. ZO proteins are further divided into 3 groups. ZO-1 plays a role in the connection between transmembrane proteins and cytoskeleton. ZO-2 is a ZO-1 homolog, able to replace ZO-1 under certain circumstances without affecting TJ formation. ZO-3 is a BCSFB-specific protein, also homologous to other ZO-proteins and able to replace their functions [26, 49, 12, 57, 20].

1.3.1.1.2. Adherens Junctions

AJ is a form of cell-cell contact were a group of proteins (such as transmembrane proteins) can be distinguished: cadherin superfamily and intracellular scaffolding proteins such as alpha-, beta- and p120-catenins. The AJ intracellular proteins bind to extracellular parts of the cytoskeleton, thereby regulating its tightness. The distance between them is approximately 10-20 nm. AJs provide physical associations between cells, regulation of the actin cytoskeleton, intracellular signaling and regulation of transcription [12, 32].

The cadherin family consists of approximately 20 proteins, some of them are located in the CNS. VE-cadherin is located in CNS endothelium. N-cadherin plays a role in eyes and brain angiogenesis. E-cadherin and cadherin-10 are located in epithelial cells, particularly in the epithelial cells of the choroid plexus as a part of AJ of BCSFB. The extracellular (EC) domain of E-cadherin contains five Ca^{2+}-binding sequences. This part is essential for cell-cell adhesion. The cytoplasmatic fragment contains two catenin-binding domains, responsible for binding to the cytoskeleton: the juxtamembrane domain that binds p120-catenin and a C-terminal region that is connected with beta-catenin [12, 32, 41].

1.3.1.2. Carrier Transport

Generally, molecular transport through a cell membrane can be classified into passive diffusion, paracellular diffusion, facilitated transport, transcytosis and active transport. Compounds which cannot pass the BCSFB by passive diffusion because of TJs, but are still required in the CSF, are carried through the membrane with the help of transporters. Transporters are also responsible for removing waste products from the CSF. In this context, all transporters are divided into uptake transporters, which transfer compounds inside the cell, and efflux transporters, which move substances outside the cell. The uptake function is usually carried out by the solute carrier (SLC) family, while efflux function is performed by the ATP-binding cassette (ABC) family against concentration gradients. At the same time some SLC transporters can act bidirectional [41, 33].

1.3.1.2.1. SLC transporters

The SLC superfamily includes 52 families and 395 proteins. The classification is based on the one hand on their amino acid homology which has to be at least 25% and on the other hand according to their function, divided into facilitated transporters, ion-coupled transporters and exchangers. They carry out the transport of monosaccharides, amino acids, monocarboxylic acids, vitamins, nucleosides, purine und pyrimidine bases, ions and amphipathic acids. One important characteristic of this protein family is the independence of ATP-hydrolysis to carry out their function. In order to perform their function, facilitated transporters use energy of electrochemical potential differences whereas ion-coupled transporters use sodium or proton gradients. Glucose transporters (GLUT), Monocarboxylate Transporters (MCTs), Amino acid transporters, Peptide Transporters, Organic Cation and Anion Transporters (OC(A)Ts) and Ion Transporters belong to this family of proteins [41, 33].

1.3.1.2.2. ABC-transporters

ABC-transporters are a huge family of proteins consisting of 7 sub-families (ABC A-G) and 48 members. They are present in most cells of the human body. In order to transport substances against concentration gradients, they use the energy of ATP-hydrolysis. The size of their cargo ranges from small ions to large polypeptides. In BCSFB only 3 sub-families are present: ABCB (P-glycoprotein (Pgp) or multidrug-resistance protein (MDR), ABCC (multidrug resistance-related proteins 1-4 (MRP) and ABCG (breast cancer-resistance protein (BCRP) [41, 33, 63, 3].

1.4. ß-trace protein (BTP)

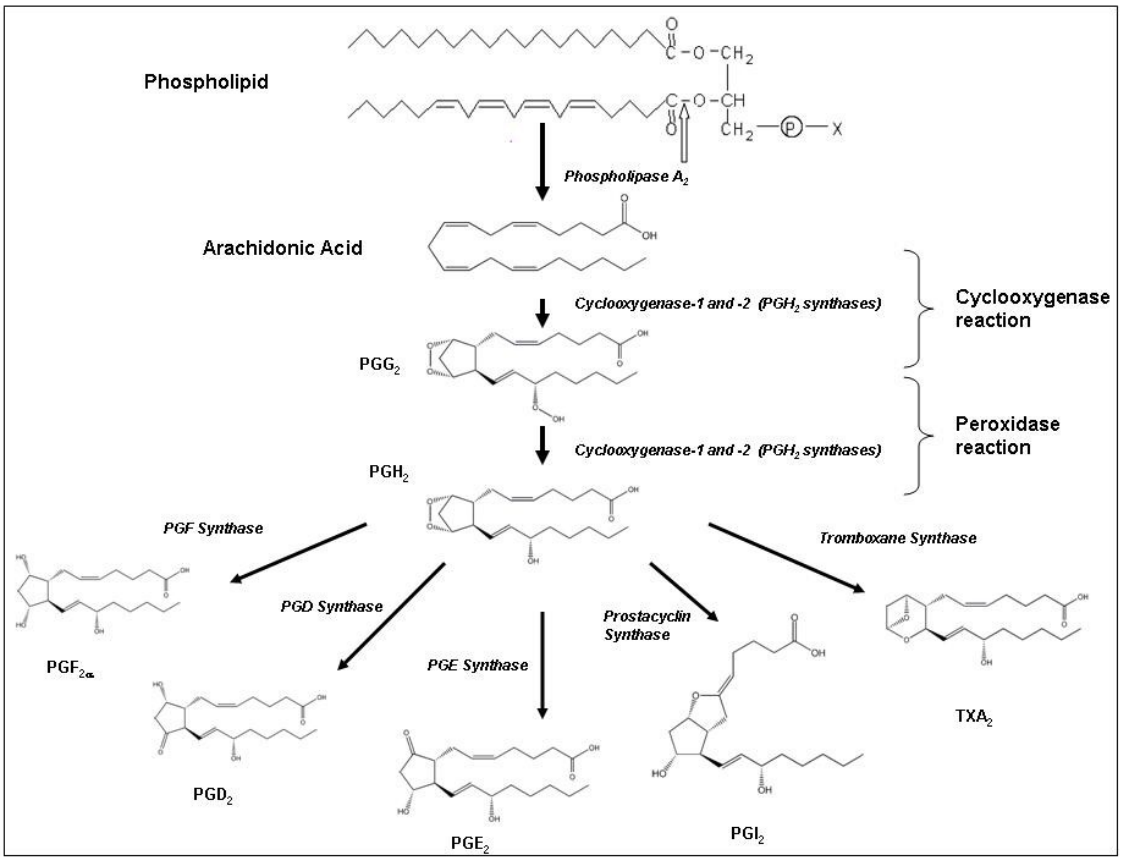

Figure 7. Place of PGD synthase in biochemical chain

Sorokin A. Glomerulonephritis and Cellular Regulation of Prostaglandin Synthesis. IntechOpen, 30.11.2011.

Since the 1990s it is known, that ß- Trace protein (BTP) carries out a prostaglandin-D synthase function [13]. Various types of eicosanoids, including prostaglandins, are produced out of open-chain, 20-carbon polyunsaturated fatty acids, typically arachidonic acid. The first step in this biochemical reaction is the enzymatically release of arachnoid acid from phospholipids in cell walls through phospholipase A2. In the second step, free arachnoid acid interacts with cyclooxygenase 1/2 (COX-1/2). The product of this reaction, PgG_2, further reacts with peroxidase, resulting in PgH_2, the direct precursor of all other types of prostaglandins. The subsequent reaction with PgH_2 prostaglandin-D synthase results in the final product, PgD_2 [55]. It acts then on many aspects of the human body, particularly in the CNS. BTP indirectly fulfills a number of different tasks [7, 54, 22, 31]:

- Sleep induction, regulation of non-rapid eye movement sleep and sedation
- Regulation of nociception
- Synapse transmission

- Hypothalamic control of temperature
- Release of lutropin
- Transport protein for biliverdin, bilirubin, retinaldehyde, retinoic acid
- Cell death prevention
- Reducing cancer progression

There are two types of PGD synthases, the hematopoetic and the lipocain enzyme. The second one is associated with the CNS [61], but so far there is contradicting literature available describing its enzymatic activity. One study revealed that BTP doesn't show the typical activity [59], however another study found that despite both types of enzymes are located in different tissues, they still show the same catalytically reaction [54]. The real range of biological functions of BTP thus still remains not fully understood.

1.4.1. Origin of production

Although most of the BTP is produced in the CNS, it can be found in other body fluids as well, however at much lower concentrations. Beside CNS there are other structures producing BTP: retina, melanocytes, male genital organs, heart, and kidney. Furthermore it is secreted into various body fluids, such as cerebrospinal fluid, seminal plasma, plasma, and urine. Depending on the BTP origin, there are notable structural differences mainly explained by different types of glycosylation. In one study different indicators were measured and compared (Table 2).

Table 2. Comparison of structural features of BTP oligosaccharides from HF, urine and CSF

	HF-BTP	Urinary-BTP	CSF-BTP
Asialo-agalacto-antennae	<2%	<2%	30%
Asialo-oligosaccharides	10%	10%	40%
Monosialo-oligosaccharides	40%	42.5%	40%
Disialo-oligosaccharides	50%	47.5%	20%
NeuAc alpha 2, 3 and alpha 2, 6	++	++	++
Bisecting GlcNAc	20%	20%	70%
Peripheral fucose (Lewis*)	<5%	<5%	20%

CNS derived BTP may be distinguished from BTP of other sources by the following features: high amounts of terminalgalactose (Gal) residues, high amounts of terminal N-acetylglucosamine (GlcNAc; agalactoantennae as well as bisecting GlcNAc), proximal alpha 1,6-fucosylation, and notable amounts of Lewis*-type peripheral fucosylation (fucose bound alpha 1,3 to GlcNAc).

A part of CNS derived BTP transfers across the BBB and BSCFB to the plasma, where it is detected by specific hepatic receptors (N-acetylglucosamine- and mannose-receptors on Kupffer and endothelial liver cells, and a Lewis-specific receptor on hepatocytes) and eliminated from the plasma [14]. At the same time, according to another study, hepatic dysfunction does not result in increased level of BTP in serum [4].

1.4.2. Concentration in CSF and affecting factors

A study in 2001 [44] showed, that the amount of BTP differs significantly in CSF of brain ventricles (V-CSF) and lumbar CSF (L-CSF). The mean concentration of V-CSF was 1.5 mg/l, while the mean concentration of L-CSF was 16.6 mg/l. This means that the concentration gradient between V- and L-CSF equals 1:11. It should be noted, that these ratios can differ for other CSF proteins (Table 3).

Table 3. Concentrations and gradients of brain-derived proteins between normal ventricular and lumbar CSF.

	NSE ng/ml	S-100 B ng/ml	Tau-Protein ng/ml	TTR mg/l	BTP mg/l	Cystatin C mg/l
V-CSF	22	5.3	0.32	17.0	1.5	0.87
L-CSF	10.8	1.5	0.21	15.3	16.6	3.1
Gradient V:L	2:1	3.5:1	1.5:1	1.1:1	1:11	1:3.5

These different results can be explained by the different dynamics of protein diffusion to the surrounding interstitium as a result of different local concentration gradients for each protein due to different origins in the CNS. Because of its leptomeningeal origin, the concentration of BTP in the lumbar part is higher than in the periventricular tissue, therefore diffusion in this region does not occur despite the higher CSF concentration.

Additionally, there is one extraleptomeningeal site of BTP production, which is located in choroid plexus but it plays a secondary role in protein synthesis in comparison to the leptomeninges. Therefore, BTP concentrations in periventricular space and ventricular cavities are lower [42, 31].

For proteins with neuronal or glial origin (NSE, S-100 B, Tau-protein) this however does not apply. Their paraventricular concentration is higher than the lumbar, due to the localization of the tissue producing these proteins. As a result, the suitable condition for diffusion in lumbar parts of the spinal cord arise and the ventricular concentration is higher than lumbar.

A few conditions can influence the concentration of BTP further:

CSF flow rate, volume

As a result of some non-inflammatory diseases, like lumbar canal stenosis, a linear increase of CSF protein content occurs, particularly BTP. This situation can be explained by constant synthesis and secretion of proteins in combination with reduced CSF flow rate [44].

Kidney parameters

BTP is a well-known and promising marker of glomerular injury and shows correlation with glomerular filtration rate (GFR). In healthy individuals BTP serum rate was 0.12-1.44 mg/l, while in patients with reduced GFRa value of 0.83-2.79 mg/l was detectable. Exceptionally high BTP values were detected in dialysis patients- in this patient group up to a mean of 8.1 mg/l BTP concentration could be detected, also affecting the serum-CSF coefficient [43, 9, 6].

Bacterial meningitis

Exclusively in bacterial meningitis the BTP level in CSF may significantly decreased down to 60%. Scientists assume two reasons of this phenomenon: Firstly, bacterial meningitis may lead to some damage of the BTP producing cells. Secondly, inflammation that accompanies the infection, results into increased permeability of the surrounded capillaries. In the latter case, levels of BTP recover within just 5 months [59, 28].

1.4.3. Practical significance

BTP is not only interesting for basic science, but also in clinical routine diagnostics to confirm or exclude CSF rhinorrhea or otorrhea, which is a pathological connection between the sinonasal cavity and the anterior or middle cranial fossae or the external ear canal, respectively.

Consequently, the weakest part of the anterior skull base is the lateral lamella of the olfactory fossa, where the bone is only 0.05 mm thin. Also, certain anatomical variations can increase the possibility of injury:

1) Position of the ethmoid roof beneath the roof of the orbit.
2) Asymmetry of the ethmoid roof.
3) Asymmetrical height of the ethmoid roof.
4) Deep position of the cribriform plate.
5) Larger angle between the skull base and the horizontal line through the sagittal plane.

The most common localizations of the lesion are:

1) Place of passage of the middle turbinate into the skull base near the A. ethmoidalis anterior.
2) Roof of ethmoid, in case of high located Sinus maxillares.
3) Central or anterior area of the ethmoidal roof.

It appears also intriguing that the right side seems to be more prone to CSF leakage [15].

CSF fistula can be generally classified into those of traumatic and non-traumatic origin. The full classification is shown in figure 8. The main cause of CSF leakage occurrence is the trauma. Accidental CSF leakage occurs as a result of blunt or penetrating face trauma. It is classified into immediate (occurs in 48 hours) and delayed CSF leakage. Up to 95% of accidental leaks are delayed. Iatrogenic leaks are a result of neurosurgical and ENT manipulations near the skull base region. In contrast, the frequency of immediate manifestation of this kind of leaks shows another picture; only in 50% of the cases the leak occurs within the first week. Non-traumatic leakages are classified as a rare event [29, 21].

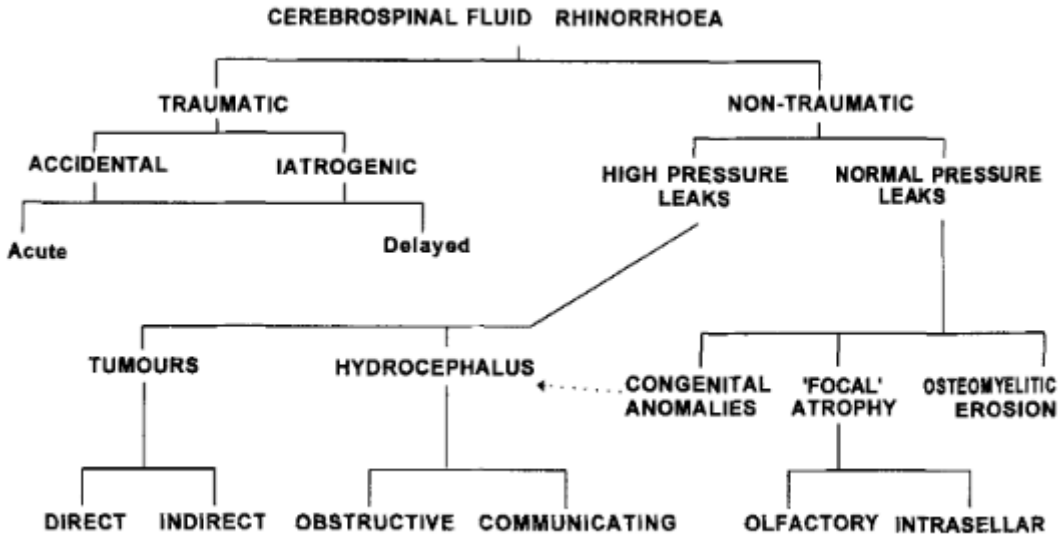

Figure 8. Classification of CSF rhinorrhea

Nandapalan V. et al. Beta-2-transferrin and cerebrospinal fluid rhinorrhoea. Clinical Otolaryngology. 1996, 21, 259-264

Additionally, spontaneous CSF leaks can be distinguished, developing without any prior known reasons. Despite this definition, there are some other factors that are related with this type of CSF rhinorrhea: idiopathic intracranial hypertension and obstructive sleep apnea, which both lead to elevated intracranial pressure [1].

The most dangerous complication of any CSF leak is the bacterial meningitis; its occurrence depends on the etiology of the leak. In general, the risk ranges from 10 to 37%. For traumatic leaks it is about 7,4% per week for the first month, 8,1% per month for the next six months and 8,4% per year after that [64]. That's why this situation requires fast diagnosis and appropriate surgical treatment.

For diagnostic purposes imaging devices, like HRCT, multidetector CT, MR imaging or MR-/CT-Cisternography can be used and have a relatively high sensitivity and specificity, of up to 92% and 100% respectively for leaks around 1 mm. However, there is still the possibility of false-positives, due to misinterpretation of findings, especially in the case of atraumatic leaks, and false-negative results, if the leak size is smaller than the detection threshold of the used method [17, 27, 62].

Laboratory studies aiming to determine CSF content in nasal secretions include measurements of glucose, beta-2 transferrin and BTP levels. Measurement of glucose level

however was determined as a weak link recently due to its low diagnostic sensitivity and specificity, caused by possible contamination from glucose-containing fluids (tears, nasal mucus, blood in nasal mucus), especially in high concentrations of blood glucose (due to Diabetes mellitus) or relatively low CSF glucose levels (due to meningitis) [5].

Beta-2 transferrin measurements show high sensitivity and specificity, from 87% and 71% respectively, up to 100%. However, there are still external factors that can influence the results: patients with alcoholism and chronic liver disease have an increased serum beta-2 transferrin level [64, 29, 11], leading to false-positive measurements in these patient groups.

BTP is the 2nd abundant protein in CSF with a relatively low serum fraction. The sensitivity and specifity appears as good as Beta-2 transferrin [42, 31, 66, 29]. All these facts make BTP an interesting target for further studies and active use in daily clinical routine for CSF rhinorrhea diagnosis. Even though BTP was discovered almost 30 years ago, it's still not widely used in clinical practice due to different issues. One of them are the undefined reference cut off values, which according to the literature range between 0.244 mg/ml and 6 mg/ml [45, 48]. Such wide ranges could be explained by methodological issues, which can significantly shift the values. Additionally, problems with the dilution of samples are frequently reported, which exceeds the detection limit and leads to exclusion of such results from final calculations [43].

2. Material and Methods

2.1. Material

In this study different types of physiological substances and patient related data were used, ventricular and lumbar liquor (n = 24 in each group), nasal discharge of known healthy volunteers (n = 17), as well as assay results of serum (n = 29) and of two groups of nasal discharge (n = 75, n = 188). All use of patient material and data has been approved by the Ethics commission of the Medical University Graz (EK 32-149 ex 19/20).

2.2. Nephelometry

2.2.1. Background

For quantitative determination of proteins in CSF, particularly BTP, nephelometry is a widely used method in laboratory routine, which belongs to Light-Scattering Assays. Key parts of the nephelometer are [10, 50]:

1) Light source. For this purpose, lamps and lasers are used.
2) Lens
3) Monochromatic system, located between radiation source and cuvette; it passes light with defined wave length.
4) Cuvette
5) The detector that catches scattered light is usually placed at different angles.
6) Analyzing system

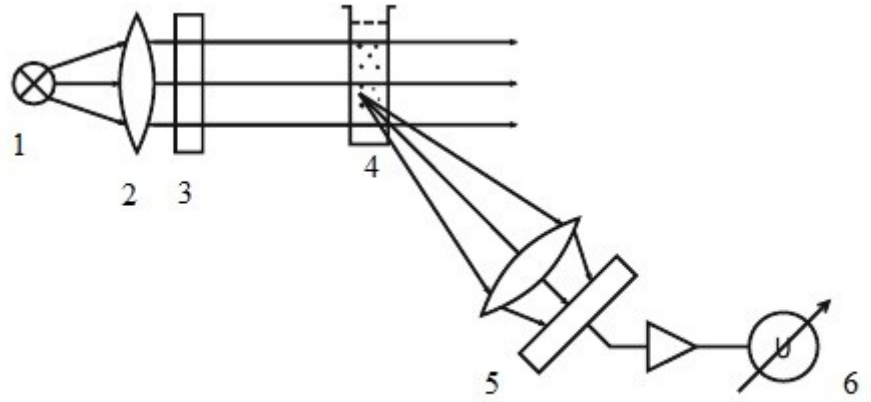

Figure 9. Schematic structure of Nephelometer

Source: Gressner A. M., Torsten A. Lexikon der Medizinischen Laboratoriumsdiagnostik, 3 Auflage, 2019. 1225-1226.

Nephelometry is based on the following interactions: The sample liquid is mixed with a reagent, consisting of latex particles coated with antibodies against the desired antigen. If the antigen is present in the investigated liquid, insoluble antigen-antibody complexes precipitate even though the affinity and avidity may differ according to antigen-antibody binding strength.

Other factors that may have an influence on the process of precipitation are:

1.) Ionic strength (high ionic concentrations decrease the strength of binding between antibody and antigen and as a result the amount of precipitate is decreased)
2.) pH (acceptable range is between 6-8)
3.) Addition of polymers (polyethylene glycol decreases solubility of immune complexes and thereby increases the amount of precipitate)
4.) Viscosity.

In a next step, the mixture is exposed to light resulting in reflection, absorption or scattering. Immune complexes, floating in the liquid, scatter the light which is measured and analyzed. The electromagnetic radiation of the light impairs the particle leading to oscillation of electrons, creating dipoles. The term dipole describes a pair of equal and oppositely charged poles separated by a distance. As a result of interactions between these charges an electric field accrue where oscillation describes the frequency of the fluctuation of the field. This field acts like a source of radiation with the same frequency and wave length as the scattered light and spreads in all directions from the particle. The strength of this dipole is also proportional to the energy of incident light, making this dipole an important source of energy for scattering. The precipitation is not a stable process and shows specific time dynamics, affecting the results. For a more accurate analysis the Heidelberger-Kendall curve is used, which can be distinguished in three parts: antibody excess, equivalence point with maximal precipitation and antigen excess. But for each reagent courses of these phases can differ. Results, which were measured up to equivalence point, are taken into account. This situation can be explained through the lattice theory, which states that precipitate forms as a result of random binding between antigens and antibodies, each antibody binds more than one antigen and vice versa. As a result of these interactions, lattice of antibody and antigen is achieved and with ongoing reaction it exceeds a critical volume of solubility. This reaction requires antigens and antibodies with at least two binding sites, in order to build chains between each other. The process of precipitation proceeds in three steps. Firstly, antigens and antibodies bind to each other and form simple complexes, corresponding to antibody excess phase; next, lattice forms (reaching equivalence point); and at last, while antigen excess, soluble complexes form [25, 30, 37, 50].

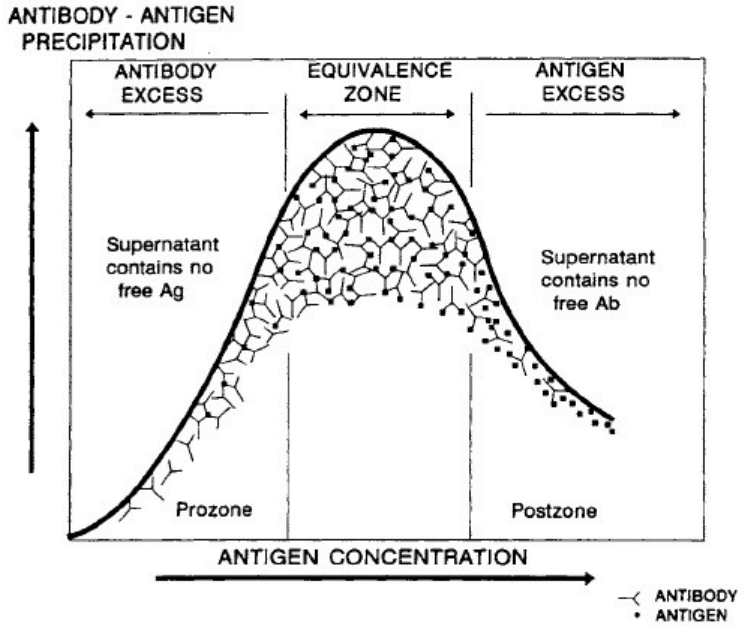

Heidelberger–Kendall immunoprecipitin curve: amount of antibody precipitated as a function of antigen concentration at fixed antibody concentration with a schematic representation of antibody–antigen complexes present in antibody excess, equivalence, and antigen excess.

Figure 10. Heidelberger-Kendall immunoprecipitin curve

Marmer D.J., Hurtubise P.E. Nephelometric and turbidimetric immunoassay. Immunoassay, 1996. 363-387

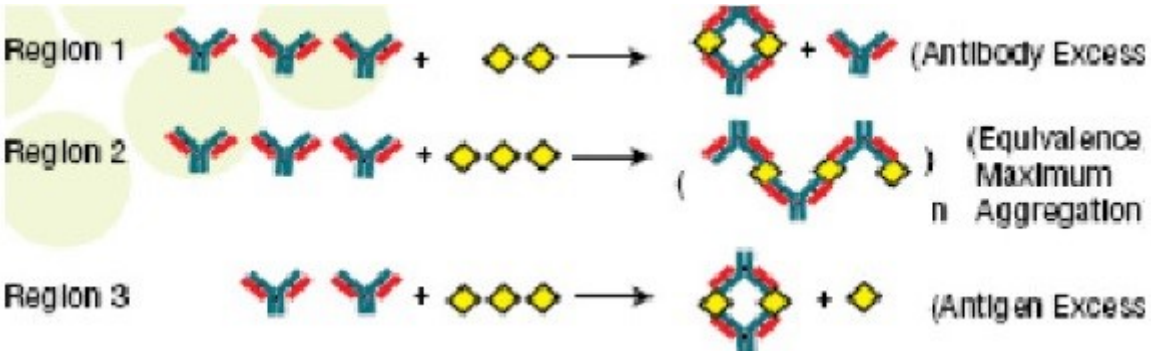

Figure 11. Schematic presentation of precipitation phases

Sasson S. Principles of nephelometry and turbidimetry focusing on IgG subclasses. Notes on Immunology, 2014.

There are two ways of performing nephelometry [50]:

1) Endpoint nephelometry: In principle, a sample is measured before and after an incubation time, reaching the so called pseudoequilibrium point. Results of the two

measurements are compared and the concentration is calculated. The main advantage of this approach is its simplicity. This assay shows a curve, displayed in Figure 12.

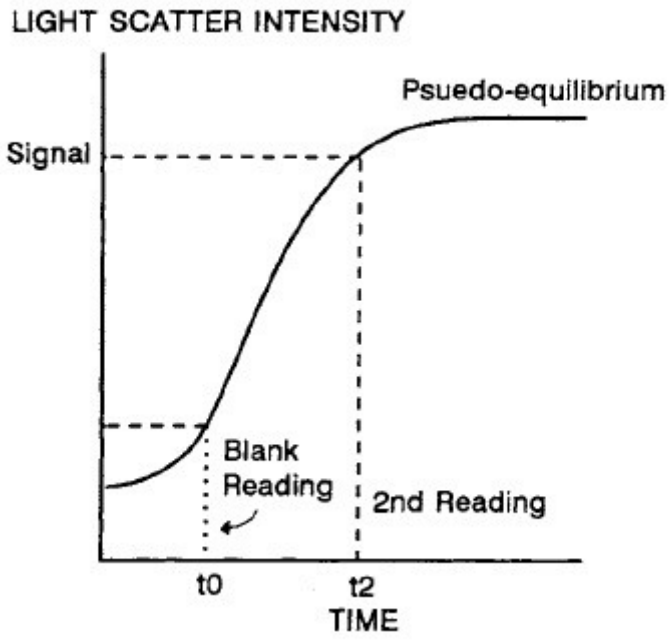

Figure 12. Points of measurements by endpoint nephelomerty

Marmer D.J., Hurtubise P.E. Nephelometric and turbidimetric immunoassay. Immunoassay, 1996. 363-387

2) Kinetic/rate nephelometry. In contrast to endpoint nephelometry, measurements are here performed constantly during the whole procedure, which can last up to one hour. It includes all periods, adding of the reagents, phases of precipitation and antigen excess phase, where calibration is performed. The aim of this method is to detect the peak concentration. This type of nephelometry is more sensitive and quicker. The curve in this case looks as depicted in Figure 13.

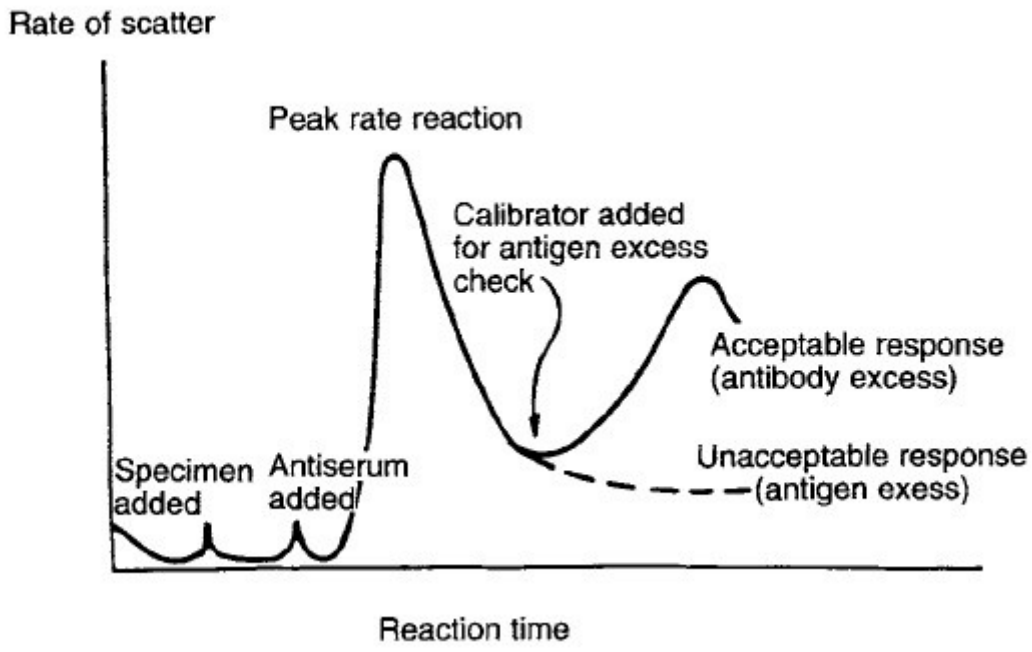

Figure 13. Curve shows changing in scattering with the time

Marmer D.J., Hurtubise P.E. Nephelometric and turbidimetric immunoassay. Immunoassay, 1996. 363-387

It is important to note that there are several factors that can also affect the procedure. The particle size should be in the wave length range of incident light; otherwise, particles won't be able to scatter the desired beam. Moreover, the size of particles determines the intensity and direction of the scattered light. If the particle is smaller than the incident wavelength, light is scattered forward, backward and in 90º. That's called Rayleigh scattering. If the particle is bigger, light scatters more forward. This pattern of scattering is called Rayleigh-Debye and both of them are characteristically for small and intermediate-size particles. Also, antigen and antibody concentrations play an outstanding role. Their concentrations result in appropriate number of immune complexes, which produce an appropriate amount of scattered light. Moreover, each device has its detection limit and if the peak concentration in one definite sample stays under or above this limit, it won't be measured. Another influencing factor is the presence of substances like chylomicrons, LDL/VLDL and other immune complexes in the investigated liquid Repeated freeze-thaw cycles, compound of suspension, refractive index of the solution, distance from incident light and angle of detection are also factors, which may affect the results [25, 30, 37, 50].

2.2.2. Conducting the Assay for measuring ß-Trace concentrations

2.2.2.1. Used Reagents

1) N Latex BTP Reagent consists of polystyrene particles loaded with rabbit antibodies against human BTP, lyophilized. It should be reconstituted with 2 mL of distillated water.
2) N Latex BTP Additional Reagent presents a rabbit immunoglobulin in buffer solution, ready for use.
3) N Protein Standard UY used for calibration.
4) N/T Protein Control LC, N Protein Control LC1, LC2 are used for control of calibration stability.
5) N Diluens is used for sample dilution.

2.2.2.2. Procedure

Material was centrifuged in Heraeus instruments Biofuge pico centrifuge for 10 minutes with 13000 rotations per minute. Then 100 µL were taken from centrifuged test tubes with an automatic pipette, mixed with 400 µL of N Diluens and placed in test tubes for the following nephelometry measurement on Beckman Coulter Image 800 Immunochemistry System.

Samples were prediluted 1:100 with N Diluens. Further steps were performed automatically. This nephelometer detects results in a range of 0.2-12 mg/L. If the BTP value is higher than 12 mg/L, samples should be additionally diluted with N Diluens or isotonic solution for further measurements and calculated respectively to assess the real ß-Trace value of the respective sample.

2.2.2.3. Experimental setup

Ventricular and lumbar CSF, pure nasal discharge of healthy volunteers and serum were analyzed using nephelometry as described above.

To simulate a laboratory model of rhinoliquorrhea, ventricular CSF was prediluted with definite ratios (pure, 2, 3 and 4 fold) and mixed with nasal discharge from healthy volunteers. These mixtures were analyzed via nephelometry to measure BTP concentrations.

2.3. Statistical Analysis

For statistical analysis, graphs, tables and charts IBM SPSS Statistics 23 and Microsoft Office 2016 were used. All groups of data are summarized in Table 4.

Table 4. Groups of used data.

Substance Type	n=
Ventricular CSF	24
Lumbar CSF	24
Nasal Discharge	17
Nasal Discharge	188
Nasal Discharge	75
Serum	29

CSF was taken from anonymized patients, nasal discharge for the experimental part from known healthy volunteers, BTP values of nasal discharge and serum were taken from previously analyzed routine clinical data.

Kolmogorov-Smirnov test was used to define the type of distribution. Since some groups revealed to be not normally distributed (ventricular CSF $p < 0.001$; serum $p < 0.001$), non-parametric tests were performed. For determining the significance between groups, Kruskal-Wallis and Mann-Whitney-U-Test was used, for investigation of correlations, Spearman's correlation coefficient was calculated.

In terms of retrospective analysis all collected samples were compared with corresponding records from surgery, whether CSF leak was found during the surgery or not. The result of comparison is presented in table 5 below.

Table 5. Groups of selected nasal discharge samples according to surgery report.

Group 1	Group 2	Group 3
53	17	5

Group 1: True positive. BTP is above cut-off value, CSF leak was determined.

Group 2: False positive. BTP is above cut-off value, CSF leak was not determined.

Group 3: True negative. BTP is below cut-off value, CSF leak was not determined.

Using these groups of data, BTP cut-off values in nasal discharge were determined via ROC Curve. Sensitivity, specificity, positive and negative predictive values were calculated with cross tables.

3. Results

In Table 6, the descriptive statistical analysis of BTP concentrations in serum and nasal discharge of previously analyzed data is presented. There is a significant difference between the two CSF types detectable ($p < 0.001$) with a higher BTP concentration in lumbar CSF (Figure 13). With a p-value of < 0.001 BTP concentration in Serum was significantly higher than in nasal discharge (Figure 14).

Table 6. Descriptive statistic of BTP concentration in different substances, mg/l.

Substance Type	Minimal Value	Maximal Value	Mean	Standard Deviation
Ventricular CSF	1.28	34.88	10.94	9.92
Lumbar CSF	9.34	45.2	25.69	11.19
Serum	0.2	1.69	0.52	0.23
Nasal Discharge	0.21	0.39	0.29	0.62

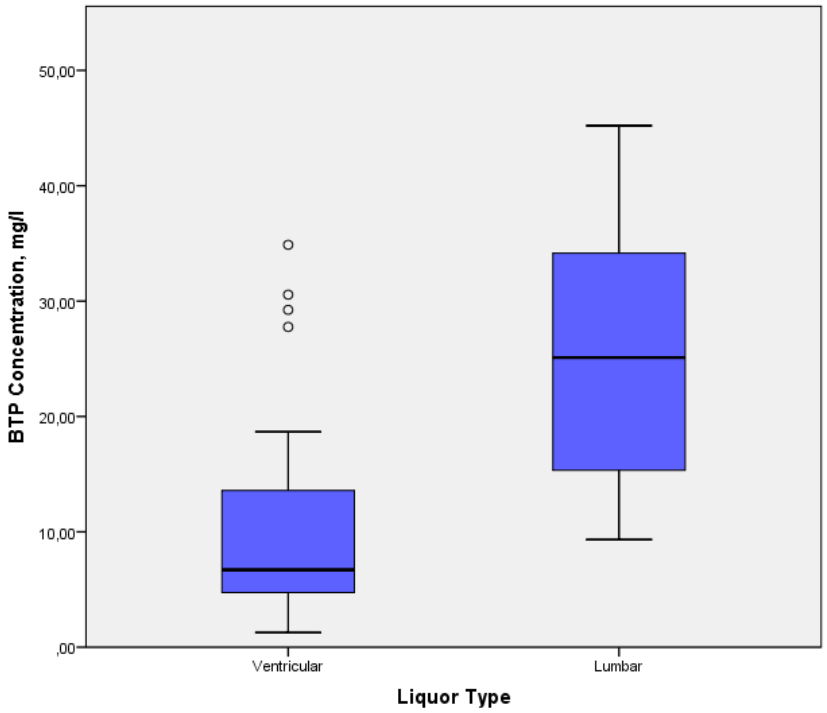

Figure 14. BTP concentrations in ventricular and lumbar CSF

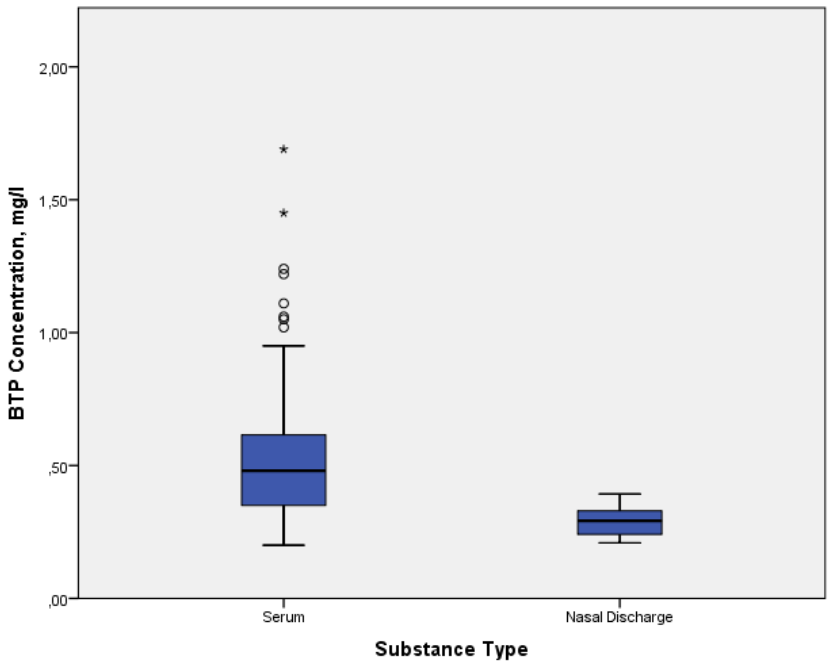

Figure 15. BTP concentrations in serum and nasal discharge

As a next step, prediluted ventricular or lumbar CSF was mixed with nasal discharge from known healthy volunteers and analyzed via nephelometry. The upper detection limit of nephelometry for BTP is 12 mg/l, therefore samples with higher concentrations have to be diluted further (considering the appropriate dilution factor to calculate the final concentration) or must be excluded. In this work 4 samples reached this detection limit and were excluded. Table 7 and Figure 15 show descriptive statistical anylysis of BTP concentration in corresponding mixtures.

Table 7. Descriptive statistic of BTP concentration in prediluted nasal discharge samples, mg/l.

Dilution rate	Minimal Value	Maximal Value	Mean	Standard Deviation
Pure	2.09	9.45	5.94	2.18
2 Fold	1.09	5.72	2.91	1.28
3 Fold	0.84	3.65	1.89	0.82
4 Fold	0.75	2.33	1.46	0.49

For estimating correlation strength Spearman's correlation coefficient was chosen. There was a significant ($p < 0.001$) inverse correlation detectable.

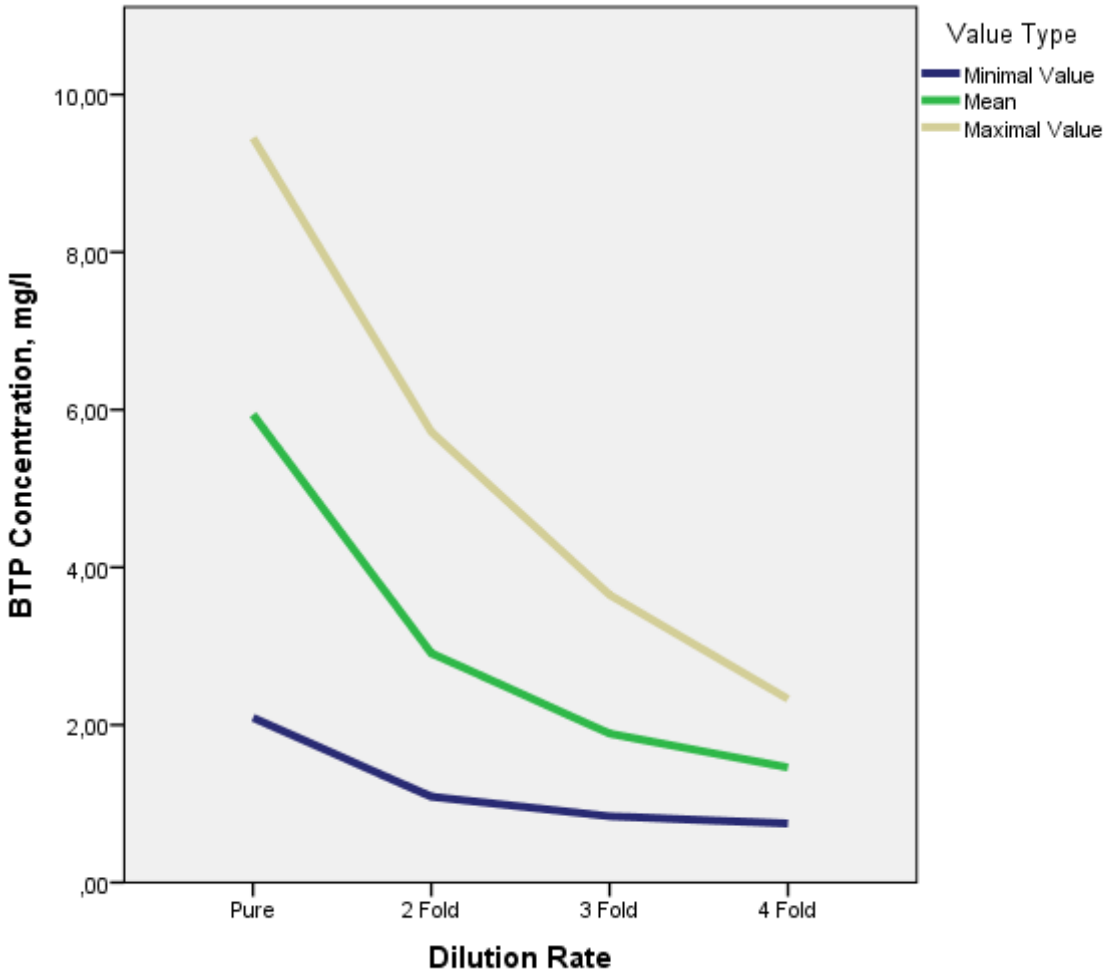

Figure 16. BTP concentrations in nasal discharge in accordance to dilution rate

The ROC curve (Figure 16) with a significance of $p < 0.001$ demonstrated an AUC of 0.765.

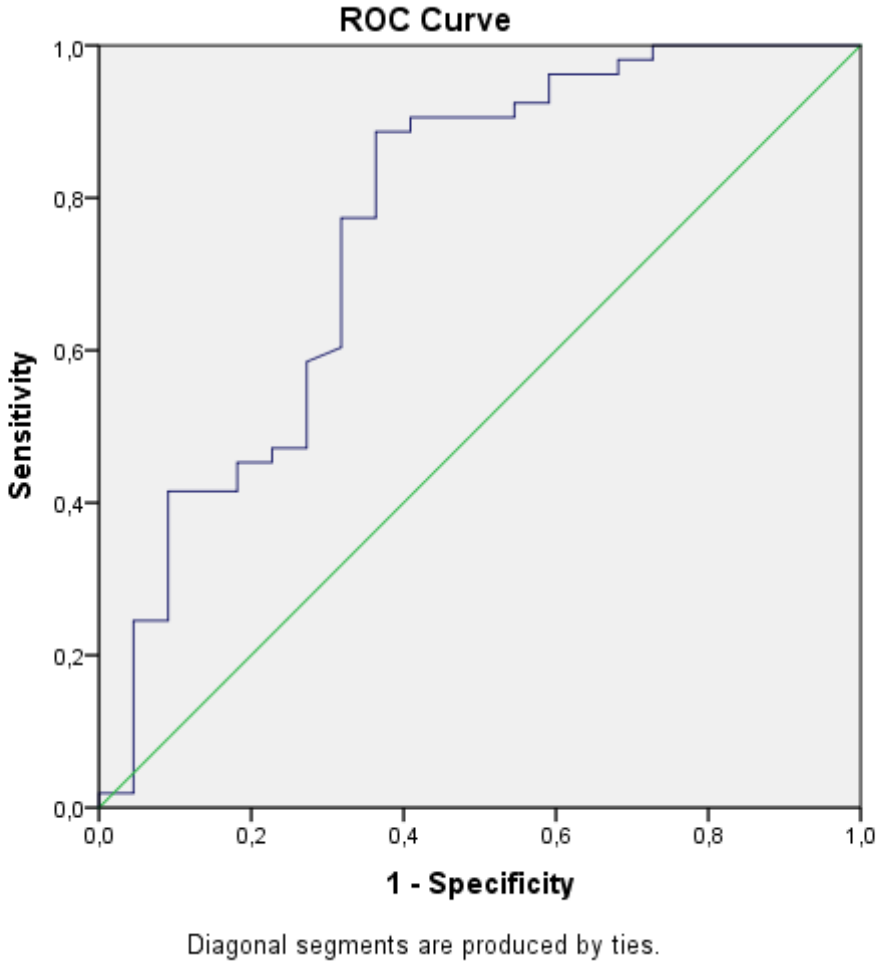

Figure 17. ROC curve of nasal discharge samples.

Retrospective analysis of previously collected samples with a significance of $p < 0.001$ revealed 100% sensitivity with a positive prediction value of 75,7% and a specificity of 22,7% with a negative predictive value of 100%.

4. Discussion

Rhinoliquorrhea is a clinical condition, characterized by the loss of CSF through the nasal cavity by a pathological connection between the anterior or middle cranial fossa with the nose. The main cause of its occurrence is a blunt trauma, non traumatical causes are considered as comparably rare [29]. The etiological classification is summarized in Figure 8.

With a risk of 1.3 % per day in first two weeks, 7.4 % per week in the first month and 8.4% per year or up to 37% during conservative treatment, the most dangerous complication of rhinoliquorrhea is bacterial meningitis. [11]. Thus an accurate and fast diagnosis is important.

Generally, the presence of CSF leaks can be confirmed by laboratory and radiological methods.

Radiological methods are mainly used for the verification of leakage localization. According to review of Gretchen M., et al. 2016, high resolution computer tomography (HRCT) is assumed as the first choice method. Magnetic resonance cisternography was considered as the second line option [11]. The main limitation for radiological methods is the leakage size. There is a correlation between leakage size and diagnostic accuracy. One study revealed the probability of 75% for detecting the leakage within 2 mm via HRCT [2].

Among laboratory analyses glucose oxidase test, Beta-2-Transferrin and BTP assays can be distinguished, however diagnostic accuracy of these methods differ.

Determining glucose admixtures in nose secretion is a fast, cheap and easy method with a detection limit of about 30 mg/dl, which is slightly below the normal CSF glucose concentration of 50-75 mg/dl [19, 66, 11]. However, a variety of limitation factors complicates the practical use of this method. Despite glucose is not detected in airway secretion of healthy individuals, local inflammation processes, blood glucose level above 121 mg/dl or contamination with substances like blood, tears and nasal mucous may lead to false positive results and reduce the sensitivity and specificity of the test [29, 11, 39]. For example, one study demonstrated 80% specificity and 0% sensitivity [5]. Another study revealed close indexes of sensitivity (1.0) and specificity (0.45) [65]. Such results do not allow to accept a glucose oxidase test as a reliable diagnostic method.

Beta-2-Transferrin appears to be a promising diagnostic tool. It is part of a polypeptide family called transferrins, responsible for iron ion transport. This family includes two types of peptides. Beside Beta-1-Transferrin, which is found in serum, nose secret, tears and saliva, there is also a CNS specific Beta-2-Transferrin described. [36]. It was suggested to predict CSF leakage in nasal discharge with especially high sensitivity and specificity. In a variety of studies those tests revealed a sensitivity from 87% to 100% and specificity from 71% to 100% [11]. However, chronical liver diseases and excessive alcohol consumption result in high transferrin concentration in plasma and may lead to false positive results [29].

BTP is an intriguing highly CNS specific protein, which can be used for diagnostic of rhinoliquorrhea. It should be noted, that BTP is also produced in organs and tissues like retina, melanocytes, male genital organs, heart, and kidney, and it is secreted into various body fluids, such as seminal plasma, plasma, and urine, but in much lesser amount. Its concentration in plasma reaches 0.54 mg/l and in nose secret 0.29 mg/l [43]. In many studies a sensitivity from 91% to 100% and a specificity from 86% to 100% were revealed [11]. With such impressive results BTP seems to be a most promising diagnostic option. However, the certain cut-off value is still not defined yet. In different studies it is suggested to accept BTP concentrations between 0.244 and 6 mg/l as a diagnostic relevant level [45, 48]. Influence factors include renal failure, changes in CSF flow rate or volume; they both lead to an increase of BTP concentration [5, 9, 43, 44]. Bacterial meningitis in contrary leads to decreased BTP values [28, 59].

Thus, the main aim of this diploma thesis is to improve the diagnostic accuracy of determining liquor leakage and performing a new evaluation of existing cut-off values in nasal discharge. As a subsidiary task, a retrospective calculation of specificity, sensitivity, NPV and PPV was performed.

From literature it is known, that BTP concentration in V-CSF and L-CSF differ with means of 1.5 mg/l and 16.6 mg/l respectively with a concentration gradient of 1:11 [42, 44]. Interestingly, our study revealed way higher values, 10.94 mg/l for V-CSF and 25.96 mgl/l for L-CSF, resulting in a concentration gradient of 1:2.37. In this regard, factors that may increase BTP concentration, such as decreased CSF flow rate and renal failure, should be taken into account [6, 9, 43, 44].

Concentrations in serum and nasal discharge of healthy volunteers showed values of 0.29 mg/l and 0.54 mg/l, comparable to already published data [43]. At the same time, analysis of serum BTP levels revealed relative high concentrations in some single samples, up to 1.69 mg/l, which can be explained by preexisting chronic renal failure [9, 6].

By adding prediluted ventricular or lumbar liquor in different rates (pure, 2-, 3- and 4-Fold) to nasal discharge of healthy volunteers, a significant inverse correlation of BTP concentration in sample and dilution rate of added liquor ($p < 0.001$) could be detected. This result could help to determine even smallest liquor admixtures surely and with a high probability of finding predicted skull base defects.

However, the retrospective analysis of previous measurements which were surgically evaluated revealed 100% sensitivity, a positive prediction value of 75.7% and a specificity of 22.7% with a negative prediction value of 100% ($p < 0.001$) using a cut-off value of 1.3 mg/ml.

Based on exploring diagnostic and treatment strategies of selected clinical cases, some factors were suggested to influence the statistical evaluation. In the majority of cases, there is a long interval (up to a month) between positive BTP analysis and operative exploration. From literature it is known, that leaks, especially small ones, can close spontaneously [69], at least temporarily.

Additionally, in some cases, the attending physician decided to use alternative therapy options instead of a direct leakage search - such cases had to be excluded from the final evaluation of this work.

Another reason could be the fact, that only a few of BTP negative patients were operatively explored, resulting in a reduced finding of false negative cases rising sensitivity and PNV to 100%.

Further, in some clinical conditions, like multiple skull injuries, serum can be admixed to the nasal discharge. In such cases of especially high serum BTP concentration, even above the current cut-off value (as shown in Figure 15) this may lead to false positive results.

In contrary, bacterial meningitis leads to low BTP concentration in CSF [59]; in this case, BTP evaluation should be postponed until acute meningitis treatment is done.

And at least, human failure cannot be excluded since anatomical conditions can be unfavorable or the leakage can be too small to be found by the surgeon. According to one study, sensitivity of endoscopic surgical investigation using intrathecal injection of sodium fluorescein ranges between 57.7% and 85.6%, with a specificity of 100% [52].

5. Conclusion

The results of this study suggest the acceptance of the current clinical index of 1.3 mg/ml as an appropriate cut-off value.

In summary, BTP seems to be a promising marker of rhinoliquorrhea for routine clinical use, which however requires further evaluation, considering the limitation factors.

6. References

1. Bakhsheshian J., Hwang M., Friedman M. Association Between Obstructive Sleep Apnea and Spontaneous Cerebrospinal Fluid Leaks: A Systematic Review and Meta-analysis. JAMA Otolaryngology – Head & Neck Surgery. 2015 Aug;141(8):733-8.
2. Baugon K. L. Imaging evaluation of the patient with a CSF leak. GSO 2013
3. Begley DJ. ABC transporters and the blood-brain barrier. Current Pharmaceutical Design, 2004. 10(12):1295-312.
4. Chakraborty B., et al. Serum BTP concentrations are not affected by hepatic dysfunction. BMC Nephrology, 2018.
5. Chan D. T., Poon W. S., Ip C. P., Chiu P. W., goh KY. How useful is glucose detection in diagnosing cerebrospinal fluid leak? The rational use of CT and Beta-2 transferrin assay in detection of cerebrospinal fluid fistula. Asian Journal of Surgery, Elsevier, 2004. 39-42.
6. Filler G., et al. Beta-trace protein as a marker of GFR—History, indications, and future research. Clinical Biochemistry. September 2014.
7. Fukuhara A, Yamada M, Fujimori K, Miyamoto Y, Kusumoto T, Nakajima H, Inui T. Lipocalin-type prostaglandin D synthase protects against oxidative stress-induced neuronal cell death. The Biochemical Journal, 2012. 443(1):75-84.
8. Garzorz N. Basics Neuroanatomie, 2008. 92-97
9. Gerhardt T., et al. Serum levels of beta-trace protein and its association to diuresis in haemodialysis patients. Nephrology Dialysis Transplantation, Volume 23, Issue 1, January 2008. 309–314
10. Gressner A. M., Torsten A. Lexikon der Medizinischen Laboratoriumsdiagnostik, 3 Auflage, 2019. 1225-1226.
11. Gretchen M., et al. Diagnosis of cerebrospinal fluid rhinorrhea: an evidence-based review with recommendations. International Forum of Allergy & Rhinology, Vol. 6, No. 1, January 2016. 8-16.
12. Hartsock A, Nelson WJ. Adherens and tight junctions: structure, function and connections to the actin cytoskeleton. Biochimica et Biophysica Acta, 2008. 1778(3):660-9.
13. Hoffmann A, Conradt S. H, Gross G, Nimtz M, Lottspeich F, Wurster U. Purification and Chemical Characterization of β-Trace Protein from Human

Cerebrospinal Fluid: Its Identification as Prostaglandin D Synthase. Journal of Neurochemistry, 1993. 451-456

14. Hoffmann A., Nimtz M., Conradt S.H. Molecular characterization of P-trace protein in human serum and urine: a potential diagnostic marker for renal diseases. Glycobiology vol. 7 no. 4, 1997. 499-506
15. Hosemann W., Draf C. Danger points, complications and medico-legal aspects in endoscopic sinus surgery. GMS Current Topics in Otorhinolaryngology - Head and Neck Surgery, 2013.
16. Javed K, Lui F. Neuroanatomy, Choroid plexus. StatPearls, 2019
17. Ji-Woong Oh, So-Hyun Kim, Kum Whang. Traumatic Cerebrospinal Fluid Leak: Diagnosis and Management. Korean Journal of Neurotrauma, 2017. 63–67
18. Johanson CE, Stopa EG, McMillan PN. The blood-cerebrospinal fluid barrier: structure and functional significance. Methods in Molecular Biology, 2011. 686:101-31.
19. Klinke R., Pape H-C. Physiologie, 5.Auflage. Georg Thieme Verlag Stuttgart, 2005
20. Kratzer I, Vasiljevic A, Rey C, Fevre-Montange M, Saunders N, Strazielle N, Ghersi-Egea JF. Complexity and developmental changes in the expression pattern of claudins at the blood-CSF barrier. Histochemistry and Cell Biology, 2012. 138(6):861-79.
21. Kruszewski W., Kruszewska K., Mantur M. Cerebrospinal rhinorrhea--etiology, clinical signs and laboratory diagnosis. Polski merkuriusz lekarski. Jul-Sep 2009;18(3):244-9.
22. Kumasaka T., et al. Structural Basis of the Catalytic Mechanism Operating in Open-Closed Conformers of Lipocalin Type Prostaglandin D Synthase. The Journal of Biological Chemistry, 2009. 22344-22352
23. Lam A, Holbrook E. Skull base anatomy and CSF rhinorrhea. Advances in Oto-Rhino-Laryngology, 2013. 74:1-11.
24. Lauren N. Telano; Stephen Baker. Physiology, Cerebral Spinal Fluid (CSF). StatPearls, 2018
25. Light-Scattering Assays, Tech Note 304. Bangs Laboratories Inc. 1999.
26. Liu WY, Wang ZB, Zhang LC, Wei X, Li L. Tight junction in blood-brain barrier: an overview of structure, regulation, and regulator substances. CNS Neuroscience & Therapeutics, 2012. 18(8):609-15.

27. Lloyd K. M., Del Gaudio J. M., Hudgins P. A. Imaging of Skull Base Cerebrospinal Fluid Leaks in Adults. Radiology: Volume 248, 2008. 725-736
28. Luissint AC, Artus C, Glacial F, Ganeshamoorthy K, Couraud PO. Tight junctions at the blood brain barrier: physiological architecture and disease-associated dysregulation. Fluids and Barriers of the CNS, 2012. 9(1):23.
29. Mantur M., et al. Cerebrospinal fluid leakage—Reliable diagnostic methods. Clinica Chimica Acta, 2011. 837-40
30. Marmer D.J., Hurtubise P.E. Nephelometric and turbidimetric immunoassay. Immunoassay, 1996. 363-387.
31. Meco C., Oberascher G., Arrer E., Moser G., Albegger K. Beta-trace protein test: new guidelines for the reliable diagnosis of cerebrospinal fluid fistula. Otolaryngology–Head and Neck Surgery, 2003. 129(5):508-17.
32. Meng W, Takeichi M. Adherens junction: molecular architecture and regulation. Cold Spring Harbor Perspectives in Biology, 2009. 1(6):a002899.
33. Morris ME, Rodriguez-Cruz V, Felmlee MA. SLC and ABC Transporters: Expression, Localization, and Species Differences at the Blood-Brain and the Blood-Cerebrospinal Fluid Barriers. The AAPS Journal, 2017. 19(5):1317-1331.
34. Mount C.A., Das J.M. StatPearls Publishing, 2020
35. Nakamura S., Maeda K., Sasaki J., Tsubokawa T. Serotonergic effect on cerebrospinal fluid production. No To Shinkei, 1985.
36. Nandapalan V. et al. Beta-2-transferrin and cerebrospinal fluid rhinorrhoea. Clinical Otolaryngology. 1996, 21, 259-264
37. Nilsson L. Nephelometry. Encyclopedia of Immunology, Second Edition, 1998. 1822-1823.
38. Patel CR, Fernandez-Miranda JC, Wang WH, Wang EW. Skull Base Anatomy. Otolaryngologic Clinics of North America, 2016. 49(1):9-20.
39. Philips B.J., Meguer J.X., Redman J., Baker E.H. Factors determining the appearance of glucose in upper and lower respiratory tract secretions. Intensive Care Medicine. 2003; 29:2204–2210.
40. Quirk B, Connor S. Skull base imaging, anatomy, pathology and protocols. Practical Neurology, 2019.
41. Redzic Z. Molecular biology of the blood-brain and the blood-cerebrospinal fluid barriers: similarities and differences. Fluids and Barriers of the CNS, 2011. 18;8(1):3.

42. Reiber H, Walther K, Althaus H. Beta-trace protein as sensitive marker for CSF rhinorhea and CSF otorhea. Acta Neurologica Scandinavica, 2003. 108(5):359-62.
43. Reiber H. Beta-trace protein concentration in nasal secretion: discrepancies and flaws in recent publications. Acta Neurologica Scandinavica, 2004. 339-341.
44. Reiber H. Dynamics of brain-derived proteins in cerebrospinal fluid. Clinica Chimica Acta, 2001. 173-186
45. Risch L., Lisec I., Jutzi M., Podvinec M., Landolt H., Huber A.R. Rapid, accurate and non-invasive detection of cerebrospinal fluid leakage using combined determination of beta-trace protein in secretion and serum. Clinica Chimica Acta, 2005. 169-76
46. Roshini S.A., David R.B., Ian R.L. Assessment of proteins of the immune system. Clinical Immunology: Principles and Practice: Fourth Edition, 2012. 1145-1159.
47. Sakka L., Coll G., Chazal J. Anatomy and physiology of cerebrospinal fluid. European Annals Otorhinolaryngology, Head Neck Diseases. 2011. 128, 309-16
48. Sampaio M.H., de Barros-Mazon S., Sakano E., Chone C.T. Predictability of quantification of beta-trace protein for diagnosis of cerebrospinal fluid leak: cutoff determination in nasal fluids with two control groups. American Journal of Rhinology & Allergy, 2009. 585-90
49. Sanchez-Covarrubias L, Slosky LM, Thompson BJ, Davis TP, Ronaldson PT. Transporters at CNS barrier sites: obstacles or opportunities for drug delivery? Current Pharmaceutical Design, 2014. 20(10):1422-49.
50. Sasson S. Principles of nephelometry and turbidimetry focusing on IgG subclasses. Notes on Immunology, 2014.
51. Sawada N, Murata M, Kikuchi K, Osanai M, Tobioka H, Kojima T, Chiba H. Tight junctions and human diseases. Medical Electron Microscopy, 2003. 36(3):147-56.
52. Seth R, Rajasekaran K, Benninger MS, Batra PS. The utility of intrathecal fluorescein in cerebrospinal fluid leak repair. Otolaryngol Head Neck Surg. 2010;143:626–32.
53. Shenoy S. S., Lui F. Neuroanatomy, Ventricular System. StatPearls Publishing, 2018.
54. Sing Mei Lim, Dan Chen, Hsiangling T., Roos A, Jansson A. E., Nyman T., Trésaugues L., Pervushin K., Nordlund P. Structural and dynamic insights into substrate binding and catalysis of human lipocalin prostaglandin D synthase. Journal of Lipid Research, 2013. 1630-1643

55. Sirois J., et al. The Ovary (Second Edition). Elsevier, 2004. 233-247
56. Steinemann A, Galm I, Chip S, Nitsch C, Maly I.P. Claudin-1, -2 and -3 Are Selectively Expressed in the Epithelia of the Choroid Plexus of the Mouse from Early Development and into Adulthood While Claudin-5 is Restricted to Endothelial Cells. Frontiers in Neuroanatomy, 2016.
57. Szmydynger-Chodobska J, Pascale CL, Pfeffer AN, Coulter C, Chodobski A. Expression of junctional proteins in choroid plexus epithelial cell lines: a comparative study. Cerebrospinal Fluid Research, 2007. 27; 4:11.
58. Tietz S, Engelhardt B. Brain barriers: Crosstalk between complex tight junctions and adherens junctions. Journal of Cell Biology, 2015. 209 (4): 493.
59. Tumani H, Reiber H, Nau R, Prange HW, Kauffmann K, Mäder M, Felgenhauer K. Beta-trace protein concentration in cerebrospinal fluid is decreased in patients with bacterial meningitis. Neuroscience Letters, 1998. 242(1):5-8.
60. Ueno M, Chiba Y, Murakami R, Matsumoto K, Kawauchi M, Fujihara R. Blood-brain barrier and blood-cerebrospinal fluid barrier in normal and pathological conditions. Brain Tumor Pathology, 2016. 3 3(2):89-96.
61. Urade U., Hayaishi O. Prostaglandin D synthase: structure and function. Vitamins and Hormones, 2000. 89-120
62. Verumi N. V., et al. Imaging review of cerebrospinal fluid leaks. Indian Journal of Radiology and Imaging, 2017. 441–446
63. Wang Q, Zuo Z. Impact of transporters and enzymes from blood–cerebrospinal fluid barrier and brain parenchyma on CNS drug uptake. Expert Opinion on Drug Metabolism & Toxicology, 2018. 14(9):961-972.
64. Warnecke A, Averbeck T, Wurster U, Harmening M, Lenarz T, Stöver T. Diagnostic relevance of beta2-transferrin for the detection of cerebrospinal fluid fistulas. Arch Otolaryngol Head Neck Surg. 2004; 1178–1184.
65. Warnecke A., Averbeck T., Wurster U., Harmening M., Lenarz T., Stover T. Diagnostic relevance of beta2-transferrin for the detection of cerebrospinalfluid fistulas. Archives of Otorhinolaryngology-Head & Neck Surgery. 2004; 130:1178–1184.
66. Welch KC. CSF Rhinorrhea. Medscape, 2018.
67. Wiegand DL, ed. AACN Procedure Manual for Critical Care. 6th ed. St Louis, MO: Elsevier Saunders; 2011.

68. Wright, Ben L. C.; Lai, James T. F.; Sinclair, Alexandra J. Cerebrospinal fluid and lumbar puncture: a practical review. Journal of Neurology, 26 January 2012. 259 (8): 1530–1545
69. Zada G., et al. Atlas of Sellar and Parasellar Lesions. Springer, 2016. 517-523